
Original article

Estimation of eruptive ages of the late Pleistocene tephra layers derived from Daisen and Sambe Volcanoes based on AMS- ^{14}C dating of the moor sediments at Ohnuma Moor in the Chugoku Mountains, Western Japan

**Shigehiro KATOH^{*1}, Kumiko HANDA^{*1}, Masayuki HYODO^{*2}, Hiroshi SATO^{*3}, Toshio NAKAMURA^{*4},
Tohru YAMASHITA^{*5} and Tohru DANHARA^{*5}**

¹⁾ *Museum of Nature and Human Activities, Hyogo; Yayoigaoka 6, Sanda, 669-1546 Japan.*

²⁾ *Research Center for Inland Seas, Kobe University; Rokkodai 1-1, Nada-ku, Kobe, 657-8501 Japan.*

³⁾ *Institute of Natural and Environmental Sciences, University of Hyogo; Yayoigaoka 6, Sanda, 669-1546 Japan.*

⁴⁾ *Nagoya University Center for Chronological Research; Furo-cho, Chikusa-ku, Nagoya, 464-8602 Japan.*

⁵⁾ *Kyoto Fission-Track Co., Ltd.; Ohmiya Minamitajiri-cho 44-4, Kita-ku, Kyoto, 603-8832 Japan.*

Abstract

The Ohnuma Moor in the eastern part of the Chugoku Mountains, western Japan, is located about 80 km west of Daisen Volcano and more than 100 km west of Sambe Volcano. The moor has thick sediments more than 63 m that are composed of peat and organic clay and clay above about 17 m in depth, and of coarser silt, sand and gravels below. The finer part contains four tephra layers of Kikai-Akahoya Volcanic Ash Beds (K-Ah), Daisen-Misen Pumice Beds (MsP), Daisen Shitano-hoki Volcanic Ash Beds (Sh), and Aira-Tanzawa Volcanic Ash Beds (AT) in descending stratigraphic order. Two volcanic ash layers are newly found in the finer sediments between K-Ah and MsP, and below AT. Based on the petrographic characteristics of the newly found two tephra layers, the upper and lower tephra layers are correlated with the upper fall unit of the Sambe Ukinuno Pumice Beds (SUK) and the Daisen Nise-hoki Volcanic Ash Beds (Nh), respectively. The eruptive ages of five tephra layers except for K-Ah are estimated using the 28 available Accelerate Mass Spectrometric ^{14}C (AMS- ^{14}C) dates obtained from the moor deposits above 17 m in depth, with the assumption of a constant sedimentation rate between the dated horizons. The resultant estimated eruption ages of SUK, MsP, Sh, AT, and Nh are $16,740 \pm 160$, $24,010 \pm 150$, $24,370 \pm 120$, $24,830 \pm 90$, and $35,650 \pm 200$ y BP, respectively. The estimated ages agree well with previous results, although the eruption age of MsP is 5,300 to 8,200 years older than the previous estimation of 16,000 to 18,500 y BP. This may result from the mismatching of tephra correlation and/or the effect of modern carbon contaminating into the materials used for the ^{14}C -age determination in the previous studies.

Key words: Tephra correlation, Accelerate Mass Spectrometric ^{14}C (AMS- ^{14}C) dating, Eruption age, Ohnuma Moor, Daisen Volcano, Sambe Volcano.

Introduction

Pliocene to middle Pleistocene volcanoes such as Mt. Hachibuse, Mt. Torokawasen, and Mt. Hyonosen are located in the eastern part of the Chugoku Mountains, northern Hyogo Prefecture (Furuyama *et al.*, 1993; Sakiyama *et al.*, 1995). In the volcanic fields, there are some highland marshes and moors like the Ohnuma, Konuma, Kosenuma, Sugigasawa, and Kahosaka Moors. The Ohnuma Moor (N35°24'28", E134°32'36") with an area of about 2 ha is located at Muraoka, Kami Town (Fig. 1), and is the largest raised mire in this prefecture (Takenaka and Kojima, 1987). The moor is surrounded by a landslide slope at the west side and by landslide blocks at other three sides. It has a gourd-shaped outline and the lowest part of the moor surface is about 810 m in altitude. This moor originates from the buried depression caused by the large-scale landslide on the northeastern slope of Mt. Hachibuse before at least 30,000 y BP (Katoh *et al.*, 2006), and the present raised mire have started to be formed since about 10,000 y BP (Miyoshi and Yano, 1986).

The northwestern part of Hyogo Prefecture is covered with Pleistocene tephra layers erupted from Daisen Volcano about 80 km west of the area, along

with the widespread tephra layers like Kikai-Akahoya (K-Ah: Machida and Arai, 1978) and Aira-Tanzawa (AT: Machida and Arai, 1976) Volcanic Ash Beds derived from calderas in southern Kyushu (Katoh *et al.*, 2001). At the eastern foot of Daisen Volcano, Shitano-hoki Volcanic Ash Beds (Sh), Odori Pyroclastic Flow Deposits (Od), Ueno-hoki Volcanic Ash Beds (Uh), Daisen Misen Pumice Beds (MsP), in ascending stratigraphic order, have been recognized in the Daisen Upper Volcanic Ash Formation above the AT horizon (Machida and Arai, 1979; Tsukui, 1984; Okada and Ishiga, 2000). Among these tephra layers, Sh and MsP were newly identified in the moor sediments at Ohnuma Moor in addition to the already found K-Ah and AT (Katoh *et al.*, 2006).

We have taken five sediment cores drilled at Ohnuma Moor in 2002 and 2003 to determine late Pleistocene paleoenvironmental changes in and around the moor. In the five cores, we have newly recognized two volcanic ash layers as well as K-Ah, MsP, Sh, and AT. In the present paper, we describe the stratigraphic positions, lithology, and petrographic properties of the two ash beds and correlate them with the Daisen Nise-hoki Volcanic Ash Beds (Nh: Okada and Tanimoto, 1986) and the upper fall unit of the Sambe Ukinuno Pumice Beds

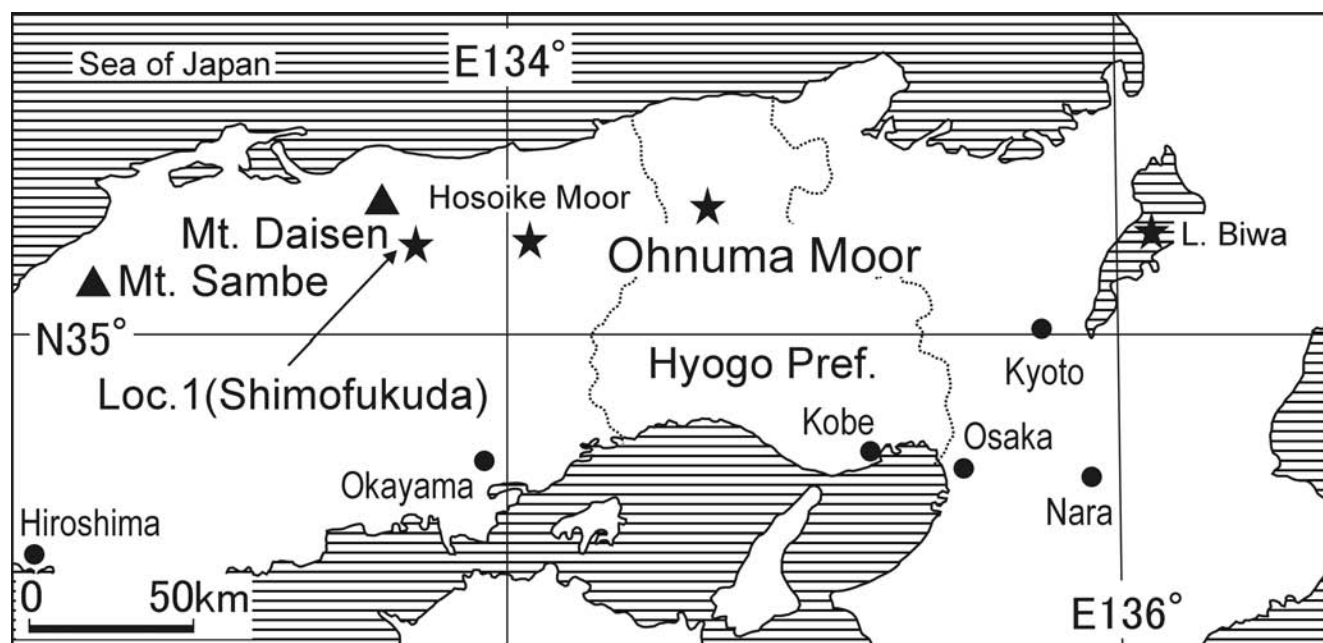


Figure 1. Localities of the Ohnuma Moor in the eastern part of the Chugoku Mountains, and of Daisen and Sambe Volcanoes. Loc.1 (Shimofukuda) is one of the type stratigraphic sections of the Daisen Upper Volcanic Ash Formation. A diamond in Lake Biwa indicates a locality of the Takashima-Oki boring site (Yoshikawa and Inouchi, 1991; 1993).

(SUK: Machida and Arai, 1992), the latter of which is also ascribed to the Sakate Volcanic Ash Beds (Sakate: Yoshikawa *et al.*, 1986) previously known as a widespread tephra layer in the northern and central Kinki District, western Japan (Machida and Arai, 1992). We also determine the eruption ages of the five tephra layers except for K-Ah on the basis of the 28 available Accelerate Mass Spectrometric ^{14}C (AMS- ^{14}C) dates obtained from the core sediments at Ohnuma Moor.

Age determination of the late Pleistocene tephra layers from Daisen and Sambe Volcanoes has been applied to proximal pyroclastic-flow deposits (Matsui and Inoue, 1970; Hattori *et al.*, 1983; Miura and Hayashi, 1991; Fukuoka, 2005) and distal tephra layers in peat or organic clay sediments (Nomura and Tanaka, 1986; Nomura *et al.*, 1995; Katoh *et al.*, 1996). However, the estimated eruption ages are slightly or in cases largely different among these studies. Moreover, the eruption ages of Nh and Sh have never been clarified. We determine more precise eruption ages of Nh, Sh, MsP, and SUK in the present paper and demonstrate the tephrochronological implications of moor sediments.

Lithology and Stratigraphy of the Core Sediments

According to Katoh *et al.* (2006), the sediments thicker than 30 m underlie the Ohnuma Moor, but they exceed 60 m at the central part of the moor having the largest width. Around the center, we obtained five all-core sediments named the OB-1 to OB-5 from November 10 to December 5 in 2002 and from June 5 to 12 in 2003 (Fig. 2). The OB-1 core recovered 24.20 m thick sediments rather close to the western landslide slope, whereas the OB-2 to OB-5 cores were drilled nearly at the moor center about 10 m northeast of the OB-1 drilling site. The OB-2 was cored up to 63.00 m in depth but could not reach to the basement andesitic rocks. The remainders were taken by the newly developed oriented sampling method (Katoh, 2005), to determine the paleomagnetic secular variation of the finer sediments. The OB-3 and OB-4 cores were sampled at sites about 1 m east of the OB-2 site and the OB-5 core was taken about 1 m west of the OB-2 site. The sediments of the OB-3 and OB-5 cores were continuously sampled from 4.50 to 16.68 m and from 3.90 to 4.93 m in depth, respectively. The

OB-4 core intermittently recovered the moor sediments from 3.87 to 5.28 m, 6.00 to 7.07 m, and 10.00 to 10.80 m in depth.

Detailed lithology of the five core sediments are given in Table 1. The core sediments at Ohnuma Moor are largely divided into seven lithostratigraphic units of **Unit I** to **Unit VII**, in descending order (Table 1 and Fig. 2). **Unit I:** Weakly and rarely decomposed peat toward 3.0-m depth intercalates a gray to brown volcanic ash layer (K-Ah) at the horizon from 2.65 to 2.88 m in the OB-1. In the OB-2 core, a lot of glass shards characteristic of K-Ah appear in the peat between 2.95 and 2.68 m in depth, but detection of its accurate fallout horizon is impossible. Many wood trunks are contained at some horizons especially from 1.0 to 1.5 m and just above and below the K-Ah.

Unit II: Dark gray to dark brownish gray organic clay, clay, and silty clay beds comprise the columnar parts from 3.0 to 9.0 m in depth (9.28 m in the OB-1), with strongly decomposed peat or peaty clay layers between 8.0 and 9.0 m. In this part, whitish gray volcanic ash beds of AT are intercalated between 7.0 and 7.4 m in depth and followed upward by the upper light grayish brown or whitish gray and lower whitish gray or pinkish white fine pumice beds less than 20 cm thick within the deposits between 6.5 and 7.0 m. The two pumice beds have been correlated with Sh and MsP of the Daisen Upper Volcanic Ash Formation in ascending stratigraphic order (Katoh *et al.*, 2006). In the OB-1 core, two gravel beds less than 25 cm thick are intercalated between 4.8 and 5.8 m.

Unit III: Dark brown, brown or light brown clay beds underlying the Unit II are up to 13.0-m depth (up to 12.45 m in the OB-1). It sparsely contains plant fragments of wood, cones, and leaves, and includes a few angular pebble to granule sized andesitic clasts at around 11.7 m in the OB-3 core.

Unit IV: Dark to light brown clay and silty clay beds with a few plant fragments continue toward 17.0-m depth in the OB-2 and OB-3 cores. The corresponding unit of the OB-1 core from 12.45 to 15.75 m consists mainly of silty and sandy clay with some thin sand and gravel layers, and very few plant fragments. The fourth unit contains more angular pebble to granule sized andesitic clasts at some horizons compared to the above unit III.

Unit V: The moor sediments between 16.95 and

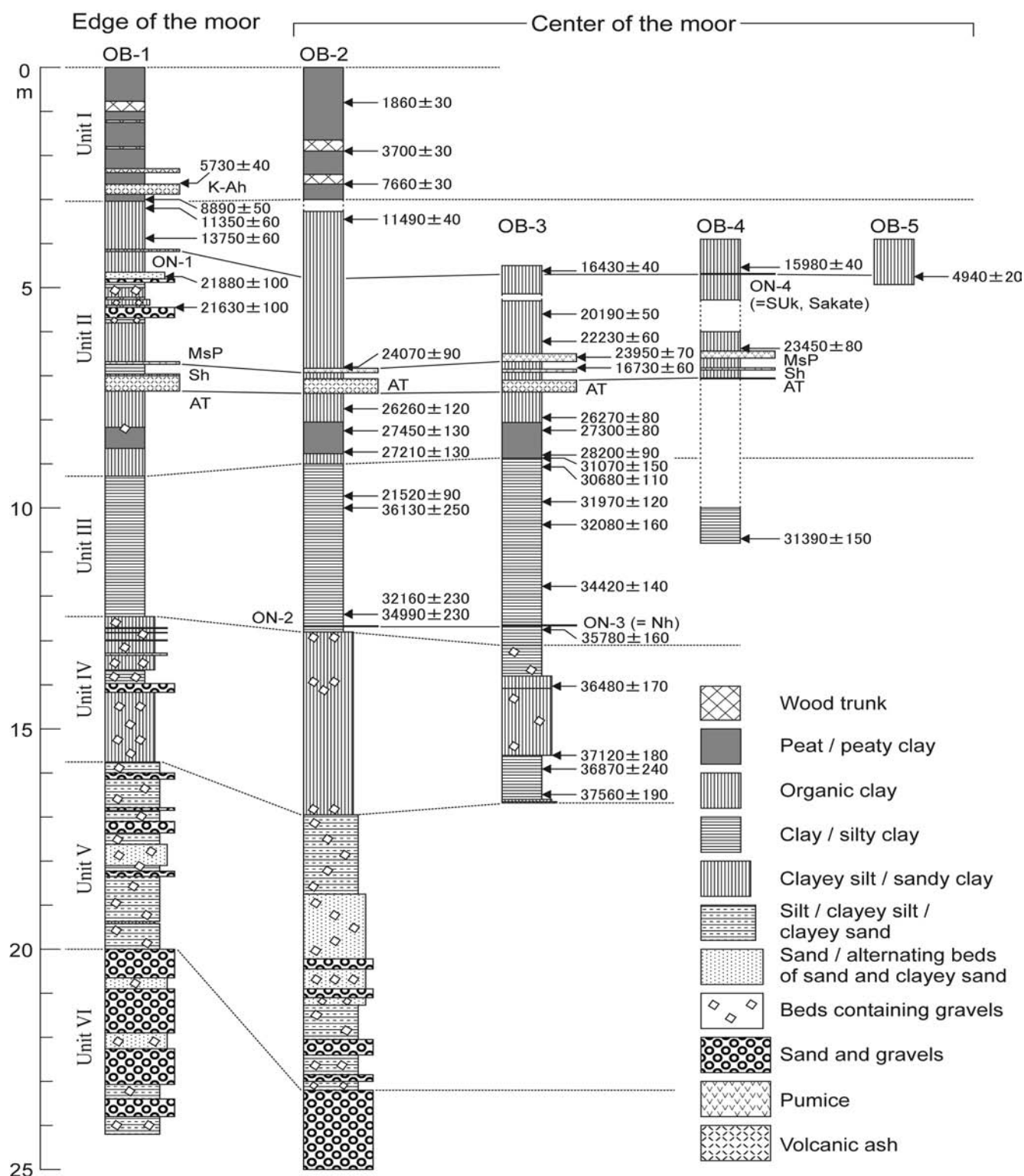


Figure 2. Geologic columnar sections of the five core sediments taken at the Ohnuma Moor with AMS-¹⁴C dates and correlated tephra layers

Tephra names and their abbreviations are after Machida and Arai (2003) for K-Ah, SUK, and AT, and after Okada and Ishiga (2000) for MsP, Sh, and Nh. K-Ah: Kikai-Akahoya Volcanic Ash Beds, SUK: Sambe-Ukinuno Volcanic Ash Beds, MsP: Daisen-Misen Pumice Beds, Sh: Daisen Shitano-hoki Volcanic Ash Beds, AT: Aira-Tanzawa Volcanic Ash Beds, Nh: Daisen Nise-hoki Volcanic Ash Beds.

Table 1. Lithology of the five drilling cores at Ohnuma Moor in the eastern part of the Chugoku Mountains, western Japan (OB-3 to OB-5 cores).

Core	Unit	Depth (m)	Thickness (m)	Color ¹⁾	Lithology
OB-3		4.50-5.14	0.64	d.gr - d.br	Organic clay partly with plant fragments of woods and leaves
		5.30	0.16		No samples
		6.50	1.20	d.gr - d.y.gr	Organic clay partly with plant fragments of woods and leaves
		6.68	0.18	w.gr	MsP ; fine pumice with visible crystals of hornblende, biotite, and feldspar.
		6.85	0.17	gr - d.y.gr	Organic clay partly with plant fragments of woods and leaves
		6.92	0.07	w.gr - gr	Sh ; coarse to medium sand sized volcanic ash with many whitish gray fine pumice grains, with visible crystals of hornblende, biotite, and feldspar.
		7.10	0.18	br - y.br	Rarely to weakly decomposed woody peat, containing many glass shards of K-Ah from 2.82 to 2.95 m in depth
		7.37	0.27	w.gr - l.gr	AT ; lowest 4cm is coarse to medium sand size volcanic ash beds including fine pumice grains, and upper 23 cm is medium to fine sand size volcanic ash beds
	II	7.59	0.22	d.y.gr	Clay including a few organic materials
		7.89	0.30	d.gr	Organic clay with a few plant fragments
		8.05	0.16	d.br	Organic clay to peaty clay with a few plant fragments like woods and cones
		8.10	0.05	d.br	Peaty clay to peat with some plant fragments including wood fragments
		8.80	0.70	d.br / bl	Moderately to strongly decomposed peat including many plant fragments like woods and leaves
		8.87	0.07	d.g.br	Peaty clay to organic clay with some plant fragments like woods and nuts, becoming blacky upwards
		9.60	0.73	d.g.br	Clay to organic clay including plant fragments like woods, leaves, cones, and nuts
		11.16	1.56	d.g.br - d.br	Clay frequently with plant fragments including woods, leaves, cones, and nuts
	III	11.65	0.49	br - d.br	Clay with a few organic materials and wood fragments
		13.10	1.45	br - d.br	Massive clay with very few wood fragments, and a few angular to sub-angular andesitic granules and pebbles at the uppermost part. Whitish gray fine pumices and hornblende crystals condensed at 12.66 to 12.64 m in depth (ON-3)
	IV	13.80	0.70	d.gr - d.br	Clay to silty clay with a few angular to sub-rounded andesitic clasts less than 10 mm in diameter, and becoming dark brown upwards
		14.08	0.28	y.gr - d.gr	Clayey silt with some angular to sub- angular weathered andesitic clasts less than 20 mm in diameter
		15.60	1.52	d.br	Clay to clayey silt with some angular to sub-rounded weathered andesitic clasts less than 20 mm in diameter and a few plant fragments, becoming darker upwards
		16.60	1.00	d.br	Massive clay to silty clay with a few plant fragments and organic materials
		16.65	0.05	gr	Clayey silt with very few organic materials and plant fragments
		16.68	0.03	gr	Sandy silt, harder relative to the upper sediments
OB-4		3.87-4.00	0.13	gr	Massive clay with very few plant fragments
		4.50	0.50	d.gr - gr	Massive organic clay with a few plant fragments
		4.70	0.20	gr	Massive clay to silty clay with a few plant fragments, intercalating a light gray to gray fine volcanic ash layer from 4.70 to 4.68 m in depth (ON-4)
		5.28	0.58	d.y.gr	Massive organic clay with a few plant fragments
		6.00	0.78		No samples
		6.44	0.44	d.g.br	Massive organic clay with a few plant fragments
		6.60	0.16	w.gr	MsP ; fine pumice with visible crystals of hornblende, biotite, and feldspar
		6.82	0.22	d.gr - gr	Silty clay with a few plant fragments
	II	6.87	0.05	w.gr	Sh ; fine pumice with visible crystals of hornblende, biotite, and feldspar
		7.05	0.08	p.w - y.gr	Tuffaceous clay to silty clay including many glass shards from AT
		7.07	0.02 +	w.gr	AT ; fine to medium sand sized volcanic ash
		10.00-10.80	0.80	d.br - br	Massive clay with a few small wood and plant fragments
	III	3.90-4.40	0.50	y.gr	Massive organic clay containing a few fine sand and silt seams, with rare plant fragments
		4.93	0.53	y.gr - d.gr	Massive organic clay with a few wood and plant fragments. Color changes upwards to gray / dark gray.

1) Color: bl, black, bl.gr, bluish gray, br, brown, d.br, dark brown, d.gr, dark gray, d.bl.gr, dark bluish gray, d.g.br, dark grayish brown, d.y.gr, dark yellowish gray, gr, gray; g.br, grayish brown, l.br, light brown, l.gr, light gray, l.g.br, light grayish brown, l.y.br, light yellowish brown, l.y.gr, light yellowish gray, p.w, pinkish white, r.br, reddish brown, w.gr, whitish gray, y.br, yellowish brown, y.gr, yellowish gray.

2) Shaded beds in the depth and thickness columns indicates coarser gravels. Depth and thickness of major tephra layers of **K-Ah**, **MsP**, **Sh**, and **AT** are shown with gothic numbers.

23.20 m in the OB-2 core are composed of the clayey sand beds including many weathered andesitic gravels and of the sandy clay matrix-supported andesitic gravels. Alternating beds of weathered andesitic gravel and dark bluish gray clayey sand dominate in the corresponding unit from 15.75 to 20.00 m in the OB-1 core.

Unit VI: This unit corresponds to the part below 20.00 m in the OB-1 and from 23.20 to 58.10 m in the OB-2, and is composed mainly of the sandy clay matrix-supported weathered andesitic gravels.

Unit VII: In the OB-2 core, the lowest unit from 58.10 to 63.00 m in depth is a weakly to moderately consolidated, and consists of gray to bluish gray sandy clay layer with some thin dark brown organic seams. The sandy clay also contains pebble to granule sized weathered andesitic clasts less frequently than in the Units V and VI.

Two tephra layers are newly recognized in the core sediments shallower than 17.0 m in addition to **K-Ah**, **MsP**, **Sh**, and **AT** (Fig. 2). Two light gray or gray fine-grained volcanic ash beds (tentatively

Table 1. (continued) Lithology of the five drilling cores at Ohnuma Moor in the eastern part of the Chugoku Mountains, western Japan (OB-2 core).

Core	Unit	Depth (m)	Thickness (m)	Color ¹⁾	Lithology
OB-2	I	1.65	1.65	br - d.br	Rarely decomposed peat with many roots
		1.90	0.30	l.y.gr	Large wood trunk (dated)
		2.43	0.53	br - d.br	Rarely decomposed peat with many wood fragments
		2.65	0.22	l.y.gr	Large wood trunk (dated)
		3.00	0.45	br - d.br	Rarely to weakly decomposed woody peat, containing many glass shards of K-Ah from 2.82 to 2.95 m in depth
	Slime	3.27	0.27	d.br - d.gr	Alternating beds of peat, wood fragments, thin volcanic ash (K-Ah glass shards). <i>Re-deposition of the upper sediments in this part after removal of the sediments by washing the boring hole.</i>
	II	6.83	3.54	gr - g.br	Organic clay to silty clay, frequently including plant fragments like woods, leaves, and cones from 3.40 to 4.00 m, from 5.00 to 6.83 m in depth
		6.93	0.10	w.gr	MsP ; coarse to medium sand sized volcanic ash with many fine pumice grains, and biotite and hornblende crystals are visible in this part
		7.05	0.12	br	Tuffaceous clay to silty clay
		7.07	0.02	l.br	Tuffaceous silty clay including many glass shards from AT
		7.22	0.15	l.g.br	AT ; fine sand sized volcanic ash
		7.30	0.08	gr	AT ; fine to medium sand sized volcanic ash
		7.40	0.10	l.y.br	AT ; medium sand sized volcanic ash
		8.05	0.65	g.br	Organic clay to silty clay, frequently containing plant fragments like woods, nuts, and cones.
		8.15	0.10	d.br	Peaty clay
		8.25	0.10	bl	Clayey peat with many plant fragments
		8.75	0.50	bl	Strongly decomposed peat with many small plant fragments
		8.77	0.02	bl	Peaty silty clay with many plant fragments
		9.00	0.23	d.br	Organic silty clay with a few plant fragments including nuts
	III	12.80	3.80	l.br - g.br	Clay to silty clay with some plant fragments mainly woods, roots, and leaves
	IV	16.95	4.15	l.gr - g.br	Clayey silt to sandy clay with angular to sub-rounded andesitic gravels mostly less than 20 mm in diameter at depths around 12.80, from 13.82 to 13.95, from 14.00 to 14.20, and from 16.70 to 16.95 m. Plant fragments mainly of small wood and root fragments and leaves are contained.
	V	18.85	1.90	gr - l.br	Clayey sand including many sub-angular to sub-rounded andesitic gravels, mostly of 10 to 20 mm in diameter and contains an andesitic boulder larger than 200 mm in diameter at 18.60 to 18.80 m
		21.27	2.42	g.br - d.gr - g.br	Alternating beds of gravels, and fine and coarse sands. Gravels dominating at 20.22 to 20.45 and 20.90 to 21.10 m in depth are mainly composed of sub-angular to sub-rounded andesitic clasts of 10 to 20 mm, partly of 50 mm in diameter.
		22.05	0.78	d.br - l.br	Clayey sand with some granule to pebble of andesitic clasts
		22.40	0.35	y.br	Sandy clay matrix-supported gravels including cobbles larger than 50 mm in diameter
		22.85	0.45	d.br	Clayey sand with some granule to pebble of andesitic clasts
		23.00	0.15	y.br	Sandy clay matrix-supported gravels including pebbles and less cobbles
		23.20	0.20	d.g.br	Clayey sand with granules
	VI	42.60	19.40	l.br / d.gr / g.br	Sandy clay matrix-supported sub-angular to sub-rounded andesitic gravels mainly of 20 to 100 mm in diameter. Thin sandy clay and clayey sand beds are intercalated at some horizons. Whitish gray and light brown weathered volcanic ash layers? (2 to 3 cm each) are intercalated at around 32.5 and 33.2 m, respectively.
		44.60	2.00	l.br - g.br	Clayey sand including some sub-angular to sub-rounded weathered andesitic gravels, mostly of 20 to 30 mm (Maximum larger than 50 mm) in diameter
		58.10	13.50	l.br / g.br / gr / bl.gr	Sandy clay matrix supported sub-angular to sub-rounded weathered andesitic gravels, frequently intercalating beds less than 0.3-m thick where sandy clay dominates. Gravels are mostly 30 to 60 mm long in diameter and sometimes those larger than 100 mm are contained.
	VII	60.50	2.40	bl.gr - gr	Moderately consolidated clay to sandy clay including weathered angular to sub-angular andesitic gravels of 50 to 100 mm in diameter
		63.00	2.50	gr / l.bl.gr / g.br	Weakly to moderately consolidated sandy clay to silty clay, partly is tuffaceous, intercalating some thin dark brown to black organic seams less than 10 mm thick

named ON-1 and ON-4) are contained at the horizons between 4.13 and 4.18 m of the OB-1 core and between 4.68 and 4.70 m of the OB-4 core, respectively (Table 1 and Fig. 2). The ash beds are rich in crystals including some phenocrysts up to 1 mm in diameter of feldspar, green hornblende, and biotite. Two volcanic ash layers of about 2 cm thick are independently recognized in the OB-2 and

OB-3 cores from 12.6 to 12.7 m in depth, and tentatively named ON-2 and ON-3 (Fig. 2). These layers are densely condensed with whitish gray very fine pumice and highly rich in green hornblende crystals. The ON-3 ash layer can be interpreted as an almost primary air-fall volcanic ash layer based on the distinct boundaries between the upper and lower clay beds.

Table 1. (continued) Lithology of the five drilling cores at Ohnuma Moor in the eastern part of the Chugoku Mountains, western Japan (OB-1 core).

Core	Unit	Depth (m)	Thickness (m)	Color ¹⁾	Lithology
OB-1	I	0.77	0.77	d.br	Rarely decomposed peat with many roots
		1.00	0.23	l.y.gr	Wood trunk
		1.20	0.20	d.br	Rarely decomposed peat
		1.25	0.05	l.y.gr	Wood trunk
		1.80	0.55	d.br-br	Rarely to weakly decomposed peat
		1.85	0.05	l.y.gr	Wood trunk
		2.65	0.80	bl	Weakly decomposed peat with many wood fragments, and white fine to medium sand sized volcanic ash grains from 2.30 to 2.39 m (Kg ?).
		2.88	0.23	gr / l.br-br	K-Ah ; lower 3cm is a gray medium to coarse sand-sized and upper 20cm is red brown to brown fine sand sized volcanic ashes
		3.00	0.12	bl	Weakly decomposed peat with clay
		3.04	0.04	d.gr	Peaty clay with many plant fragments including woods
	II	4.65	1.61	gr	Organic silty clay to clay, sparsely with plant fragments and a wood trunk (dated) at 4.50m, gray to light gray fine volcanic ashes condensed between 4.18 and 4.13 m in depth (the sample ON-1)
		4.80	0.15	br - d.gr	Fine sand with sub-angular to angular andesitic gravels less than 5 mm in diameter, including a wood fragments (dated) at 4.75m
		4.88	0.08	br - d.gr	Gravels with silty clay matrix, composed mainly of weathered angular andesitic pebbles, rarely with cobbles larger than 50 mm in diameter, with wood and plant fragments
		5.00	0.12	br	Clay with wood and plant fragments, and a few weathered angular andesitic clasts less than 10 mm in diameter
		5.22	0.22	gr	Organic clay with very few weathered angular to sub-angular andesitic clasts less than 10 mm in diameter
		5.27	0.05	br - d.gr	Wood trunk
		5.40	0.13	br	Sandy clay sparsely with sub-angular to sub-round andesitic clasts less than 10 mm in diameter
		5.45	0.05	br	Wood trunk (dated)
		5.68	0.23	g.br	Weathered sub-angular to sub-rounded andesitic gravels with clay matrix, containing cobbles larger than 50 mm in diameter
		5.80	0.12	gr	Clay sparsely with angular andesitic gravels (a maximum diameter larger than 20 mm)
		6.68	0.88	d.gr / gr / l.g.br	Massive organic clay with very few plant fragments
		6.74	0.06	l.g.br	MsP ; fine pumice to coarse volcanic ash with visible minerals like biotite, hornblende, and feldspar
		6.96	0.22	l.g.br	Massive clay with a few plant fragments
		7.00	0.04	p.w	Sh ; Clayey volcanic ash with many white fine pumice grains
		7.35	0.35	w.gr	AT ; medium to fine sand sized volcanic ash with some white pumice grains at its uppermost part
		7.60	0.25	l.br - l.g.br	Massive clay with a few plant fragments
		8.17	0.57	l.br	Alternating beds of organic clay and decomposed peat seams, becoming dark downwards
		8.60	0.43	d.br	Strongly decomposed peat, with a weathered angular andesitic gravel with a diameter of 50 mm at 8.20 m
		8.65	0.05	d.br	Peaty clay
		9.28	0.63	g.br	Massive organic clay with very few plant fragments, and a insect fossil. The lower boundary is clear.
	III	10.00	0.62	l.br	Massive clay with a few plant fragments, relatively harder than the above sediments
		11.05	1.05	d.br	Massive clay with very few plant fragments
		12.45	1.40	l.br	Massive clay to silty clay with a few plant fragments, becoming dark brown in color upwards
	IV	13.66	1.21	d.br	Massive sandy clay with a few weathered sub-angular to sub-rounded andesitic gravels of 2 to 20 mm in diameter. Fine to medium sand beds are intercalated between 12.70-12.72 m, 12.81-12.82 m, 12.98-13.00 m, and 13.28-13.33 m.
		13.97	0.31	l.br - d.br	Massive silty clay with very few weathered angular andesitic gravels of 5 to 10 mm in diameter
		14.17	0.20	l.br	Gravels mostly composed of angular andesitic clasts less than 20 mm in diameter, including a large boulder larger than 170 mm in diameter
		15.75	1.58	l.br - d.g.br	Massive silty clay to clayey silt commonly with a few sub-angular to sub-rounded andesitic clasts less than 10 mm in diameter and sparsely with plant fragments
	V	16.00	0.25	d.bl.gr	Clayey sand containing angular andesitic clasts less than 10 mm in diameter
		16.14	0.14	g.br	Gravels mostly of sub-angular to sub-rounded andesitic clasts, including a large cobble larger than 50 mm in diameter
		16.79	0.65	d.bl.gr	Upward fining clayey sand containing sub-angular to sub-rounded andesitic clasts less than 10 mm in diameter
		16.85	0.06	d.gr	Clast-supported gravels mainly of sub-angular andesitic pebbles less than 20 mm in diameter
		17.10	0.25	d.bl.gr	Upward fining clayey sand to clayey silt, frequently containing sub-angular to sub-rounded andesitic clasts less than 10 mm in diameter
		17.36	0.26	d.gr	Sub-angular to sub-rounded andesitic gravels with sandy clay matrix, most of gravels less than 20 mm in diameter
		17.62	0.36	d.bl.gr	Clayey sand sparsely with sub-angular to sub-round andesitic clasts less than 20 mm in diameter
		18.10	0.48	d.bl.gr	Alternating beds of medium to fine sand and clayey sand, containing some sub-angular to sub-rounded weathered andesitic clasts mostly less than 20 mm in diameter
		18.23	0.13	d.bl.gr	Clayey sand with sub-angular to sub-rounded andesitic granules
		18.35	0.12	d.bl.gr	Coarse sand and sub-angular to sub-rounded andesitic gravels, clast-supported
		19.00	0.65	d.bl.gr	Clayey sand to clayey silt with a few sub-angular to sub-rounded andesitic clasts less than 5 mm in diameter
		20.00	1.00	d.bl.gr	Clayey sand with angular to sub-rounded weathered andesitic clasts, intercalating pure sandy clay bed from 19.37 to 19.42 m in depth
	VI	20.65	0.65	d.gr	Upward fining sandy clay matrix-supported gravels, mostly of angular to sub-angular weathered andesitic clasts less than 30 mm in diameter
		20.90	0.25	d.gr	Fine sand with a few angular weathered andesitic clasts less than 20 mm in diameter
		21.90	1.00	d.gr	Sandy clay matrix-supported gravels, mostly of angular to sub-angular weathered andesitic clasts less than 50 mm in diameter, with a larger boulder of at least 100 mm in diameter
		22.26	0.36	d.gr	Clayey sand sparsely with angular andesitic clasts less than 20 mm in diameter
		23.07	0.81	d.gr - d.bl.gr	Sandy clay matrix-supported gravels, mostly of angular to sub-angular weathered andesitic clasts less than 20 mm in diameter, with a larger boulder of at least 70 mm in diameter
		23.40	0.33	br	Clayey sand including angular to sub-angular weathered andesitic clasts of 2 to 20 mm in diameter
		23.80	0.40	l.g.br	Sandy clay matrix-supported gravels, mostly of angular to sub-rounded weathered andesitic clasts larger than 50 mm in diameter, with the largest boulder of at least 220 mm in diameter
		24.20	0.40	r.br - br	Upward fining clayey sand including angular to sub-angular weathered andesitic clasts less than 50 mm in diameter

Table 2. AMS- ^{14}C dates obtained for the Ohnuma Moor sediments.

Sample No.	Core No.	Depth (m)	Material	$\delta^{13}\text{C}$ (‰)	Conventional ^{14}C Age (y BP)	Lab. Code	Calibrated Calendar Age (cal. BP)
1	OB1	2.63	peat	-23.8	5,730 \pm 40	IAAA-52833	6,540 \pm 60
2	OB1	3.00	peat	-20.4	8,890 \pm 50	IAAA-52834	10,030 \pm 100
3	OB1	3.20	wood	-21.9	11,350 \pm 60	IAAA-52835	13,250 \pm 120
4	OB1	3.88	wood	-19.6	13,750 \pm 60	IAAA-52836	17,160 \pm 140
5	OB1	4.50	wood	-27.2	21,880 \pm 100	Beta-215474	26,500 \pm 430
6	OB1	5.45	wood	-28.1	21,630 \pm 100	Beta-215475	26,210 \pm 570
7	OB2	0.80	peat	-26.6	1,860 \pm 30	NUTA2-7102	1,800 \pm 50
8	OB2	1.90	wood trunk	-24.9	3,700 \pm 30	NUTA2-7103	4,050 \pm 40
9	OB2	2.65	wood trunk	-25.4	7,660 \pm 30	NUTA2-7104	8,460 \pm 40
10	OB2	3.45	plant fragment	-28.9	11,490 \pm 40	NUTA2-7101	13,400 \pm 120
11	OB2	6.80	wood	-24.5	24,070 \pm 90	NUTA2-7105	28,960 \pm 340
12	OB2	7.75	wood	-25.5	26,260 \pm 120	NUTA2-7108	30,940 \pm 170
13	OB2	8.25	wood	-26.5	27,450 \pm 130	NUTA2-7109	31,760 \pm 350
14	OB2	8.73	peat	-28.5	27,210 \pm 130	NUTA2-7110	31,450 \pm 170
15	OB2	9.73	wood	-26.3	21,520 \pm 90	NUTA2-7111	25,730 \pm 380 *
16	OB2	10.00	plant fragment	-24.4	36,130 \pm 250	PLD-1977	41,860 \pm 190 *
17	OB2	12.40	root	-22.2	32,160 \pm 230	PLD-1978	37,630 \pm 810 *
18	OB2	12.40	wood	-25.3	34,990 \pm 230	NUTA2-7112	40,660 \pm 800
19	OB3	4.62	wood	-24.5	16,430 \pm 40	NUTA2-9682	19,720 \pm 240
20	OB3	5.60	cone	-25.5	20,190 \pm 50	NUTA2-9678	24,120 \pm 280
21	OB3	6.22	cone	-25.2	22,230 \pm 60	NUTA2-9679	26,780 \pm 430
22	OB3	6.58	wood	-24.9	23,950 \pm 70	NUTA2-9687	28,870 \pm 330
23	OB3	6.82	wood	-35.9	16,730 \pm 60	NUTA2-9688	19,960 \pm 290 *
24	OB3	7.95	cone	-25.3	26,270 \pm 80	NUTA2-9680	30,950 \pm 150
25	OB3	8.24	peat	-28.3	27,300 \pm 80	NUTA2-9689	31,520 \pm 190
26	OB3	8.80	peat	-28.5	28,200 \pm 90	NUTA2-9681	32,720 \pm 620
27	OB3	8.87	wood	-27.9	31,070 \pm 150	NUTA2-10833	36,190 \pm 260
28	OB3	9.07	nut	-25.4	30,680 \pm 110	NUTA2-9690	35,840 \pm 260
29	OB3	9.86	nut	-24.4	31,970 \pm 120	NUTA2-9691	36,900 \pm 230
30	OB3	10.38	wood	-29.0	32,080 \pm 160	NUTA2-10834	37,030 \pm 270
31	OB3	11.78	wood	-25.2	34,420 \pm 140	NUTA2-9692	40,370 \pm 710
32	OB3	12.75	root ?	-25.9	35,780 \pm 160	NUTA2-9694	41,720 \pm 170
33	OB3	14.03	wood	-28.5	36,480 \pm 170	NUTA2-9683	41,990 \pm 190
34	OB3	15.60	root ?	-28.1	37,120 \pm 180	NUTA2-9684	42,240 \pm 210
35	OB3	15.91	wood	-27.8	36,870 \pm 240	NUTA2-10835	42,130 \pm 210
36	OB3	16.49	wood	-25.5	37,560 \pm 190	NUTA2-9695	42,460 \pm 260
37	OB4	4.54	wood	-25.6	15,980 \pm 40	NUTA2-9674	19,200 \pm 180
38	OB4	6.38	wood	-26.4	23,450 \pm 80	NUTA2-10830	28,240 \pm 250
39	OB4	10.70	wood	-23.7	31,390 \pm 150	NUTA2-10831	36,420 \pm 270 *
40	OB5	4.75	wood	-22.7	4,940 \pm 20	NUTA2-9675	5,670 \pm 40 *

1) Background of the samples from the OB2 to OB5 cores was corrected using the results of rod graphite prepared at the Center for Chronological Research, Nagoya University.

2) The $^{14}\text{C}/^{12}\text{C}$ ratios of the samples from the OB2 to OB5 cores were calculated using the results of 6 standards (Hox-II) prepared by the Center for Chronological Research, Nagoya University.

3) The $\delta^{13}\text{C}$ correction from the OB2 to OB5 cores was conducted based on the values measured by Tande-II.

4) Radiocarbon dates of all samples were calculated using the Libby half-life 5,568 years.

5) All conventional ^{14}C ages were calibrated to calendar ages (cal. BP) using CalPalA-University of Cologne Radiocarbon Calibration Program in quickcal 2005 ver.1.4 (<http://www.calpal.de>).

6) Ages with asterisks were excluded in determining sedimentation rates and the eruption ages of tephra layers, because they are much younger than those estimated from their stratigraphy relative to the tephra layers and other radiocarbon dates.

Methods and Results

Accelerate Mass Spectrometric ^{14}C (AMS- ^{14}C) dating

Plant fragments of wood trunks, leaves, roots, cones and nuts, and peat were carefully sampled from the core sediments of OB-1 to OB-5 taken at the Ohnuma Moor for Accelerate Mass Spectrometric ^{14}C (AMS- ^{14}C) dating. The AMS- ^{14}C dates of the materials were measured for 32 horizons of the OB-2 to OB-5 cores using the Tandem II accelerate mass spectrometer at the Center for Chronological Research, Nagoya University (Table 2 and Fig. 2). In the OB-2 core, two AMS- ^{14}C samples from the sediments of 10.00 m and 12.40 m in depth were processed by the Paleo Labo Co., Ltd. Six AMS- ^{14}C dates of the samples in the OB-1 core were determined by Beta Analytic Inc. or Institute of Accelerator Analysis Ltd. These AMS- ^{14}C ages were corrected for ^{13}C isotopic fractionation. All the conventional radiocarbon ages were calibrated to calendar ages (cal. BP) using CalPalA-University of Cologne Radiocarbon Calibration Program Package ([http:// www.calpal.de](http://www.calpal.de)).

Petrographic Properties of newly found tephra layers

Petrographic properties such as grain and heavy mineral compositions and classification of glass shard morphology, were analyzed for the ON-1 to ON-4 volcanic ash layers following Katoh *et al.* (2001). Morphological types of glass shards were classified into H-, C-, T-types, and other types based on the criteria proposed by Yoshikawa (1976). Refractive indices of volcanic glass shards and heavy mineral phenocrysts were measured using the Refractive Index Measuring System (RIMS) 86 or RIMS 2000 (Danbara *et al.*, 1992) according to Danbara (1993) and Kamata *et al.* (1994). Refractive indices of more than 30 grains were determined for glass shards (n_1) and for orthopyroxene (n_2), hornblende (n_2), and cummingtonite (n_2). Errors in measurement are estimated to be ± 0.0002 for glass shards and ± 0.0005 for heavy and light minerals (Danbara, 1993). We describe below the petrographic properties of four tephra layers from ON-1 to ON-4 (Table 3 and Fig. 3).

In addition to the visible tephra layers of ON-1 to ON-4, we define the volcanic ash horizons corresponding to the ON-1 and ON-4 volcanic ash layers in the OB-2, OB-3, and OB-5 cores. A sediment sample of dry weight of 2 to 3 g was taken at a given interval from 4.54 to 4.99 m in the OB-2, from 4.54 to 5.02 m in the OB-3, and from 4.02 to 4.93 m in the OB-5 core. It was washed in an ultrasonic bath and then sieved to obtain a sand fraction. The sand fraction was dried at 60 °C for 6 hours to measure the weight, and calculated the weight percent of the sand fraction to the total dry weight. Grain and heavy mineral compositions, and morphology of contained glass shards were also analyzed through the same procedures as used for the visible tephra layers.

1) ON-1 (4.13-4.18 m in the OB-1 core, 5 cm thick) and ON-4 (4.68-4.70 m in the OB-4 core, 2 cm thick)

These light gray or gray fine-grained volcanic ash beds mainly consist of light mineral phenocrysts, volcanic glass shards, and glassy pumiceous rock fragments with around 10 % heavy mineral grains. A few quartz grains are included in the light minerals. Clear T-type glass shards and some other type shards are dominant. Contained are a small amount of H-type shards but they are considered to be derived from AT. Pale-gray to pale-brown blocky glass shards that sometimes include microlite crystals of feldspar, quartz, and heavy minerals are richest in other type shards. Pale-brown or brown very fine-bubbled shards are also common in other types and include microlite crystals. Refractive indices (n) of the clear T-type and other type glass shards in ON-1 and those of the clear T-type glass shards in ON-4 are 1.498-1.500 (mode: 1.499) and 1.496-1.501 (1.499), respectively. Heavy minerals are mostly composed of green hornblende (77 - 78.5 %), cummingtonite (7.5 - 8.5 %), and opaque minerals (7 - 8.5 %), and include apatite, biotite, brown hornblende, and orthopyroxene crystals less than 5 % each. In ON-4, refractive index (n_2) of most of green hornblende grains is 1.672-1.680 (1.675-1.676), although very few green or pale-brown hornblende crystals have higher refractive index of 1.687-1.691. Glass shard fragments often stick on the green hornblende phenocrysts in both ashes, while the other hornblende crystals have no glass shard cover. Cummingtonite phenocrysts are

Table 3. Petrographic properties of newly identified tephra layers intercalated with the Ohnuma Moor and their correlatives

Tephra No. (Core/Locality)	Sample ID	Depth (m)	Grain composition (%)					Heavy mineral composition (%)										Glass-type composition (%)				Refractive index (mode)		
			Gl.	Rf.	Lm.	Hm.	Ot.	Opx	Cpx	BHb	GHb	Cum	Opq	Zr	Bt	Ap	H	C	T	Oth	n : Glass	γ : Opx	n ₂ : Gho(upper), Cum(lower)	
ON-1 (OB1)	B1 418	4.18	40	14.5	34.5	11.0	0	5	0	2	77	8.5	7	0	0.5	0	12.5	9	25.5	53	1.498–1.500 (1.499) (T>Oth)	–	–	
ON-4 (OB4)	B4 470	4.70	23.5	21	47	8.5	0	1	0	1	78.5	7.5	8.5	0	1.5	2	3	1.5	78	17.5	1.496–1.501 (1.499) (T)	–	1.672–1.680 (1.675–1.676) 1.687–1.691 1.661–1.667 (1.663)	
Sakate (Nara basin) Sakate (Takashima–Oki) SUK (Pumice) ³⁾ U ₁ ³⁾ (Ukinunolike) U ₁ ³⁾ (Kobe) SUK ⁴⁾ (Hosolike Moor B2)	N4U ¹⁾	–	12	–	49	38	–	0	0	–	98	–	2	0	1	0	2	49	36	4	1.498–1.503 (1.500)	–	–	
	BT6 ²⁾	4.76	58	9	25	8	–	0	0	–	75	–	8	0	16	*	2	38	39	21	1.498–1.501 (1.498–1.500)	–	–	
	–	–	–	–	–	–	–	0	0	0	86	0	12	*	*	2	C+T				1.503–1.505 (1.504) 1.501–1.505 (1.504), 1.509	–	1.672–1.678 (1.675) 1.671–1.680 (1.675) 1.662–1.667 (1.663–1.666)	
	–	–	–	–	–	–	–	0	0	0	*	80	2	12	*	3.5	2.5	C+T				–	1.671–1.676 (1.674) 1.661–1.666 (1.664) 1.671–1.675 (1.672)	
	A	–	25	–	35	41	–	0	0	0	*	81	6	6	*	6	*	T				1.500–1.506 (1.501–1.504) 1.498–1.506 (1.502)	–	–
ON-2 (OB2)	B2 1268	12.68	*	52.5	39	8	0	18.5	*	*	70	1.5	3.5	1	1.5	3.5	34.5	9	34.5	22	1.494–1.501 (1.499)	1.694–1.703 1.707–1.710 (1.707)	1.670–1.683 (1.679–1.680) 1.685–1.691 1.660–1.665 (1.662)	
ON-3 (OB3)	B3 1266	12.66	*	37.5	55.5	6	*	6	*	1	82.5	1	3.5	0	2	3.5	*	*	*	+++	1.494–1.502 (1.500)	1.699–1.703 1.706–1.707 1.709–1.715 (1.712)	1.672–1.686 (1.677) 1.691–1.695 1.660–1.664 (1.662)	
SI (Takashima–Oki)	BT15 ²⁾	14.69	55	2	29	14	–	*	0	–	66	–	9	0	23	2	1	11	88	*	1.499–1.506 (1.499–1.501)	–	–	
Nh-U (Shimofukuda)	Nh-U	–	22	31	31.5	14.5	1	9.5	*	2.5	53.5	3	29	*	1	*	1	1	5	93	1.495–1.500 (1.498)	1.700–1.705 (1.703)	–	
Nh-M (Shimofukuda)	Nh-M	–	22	12.5	46.5	18.5	0	2	*	*	67.5	4.5	19.5	0	2	3	*	1.5	4.5	94	1.496–1.500 (1.499)	1.699–1.706 (1.702–1.703)	1.672–1.678 (1.675–1.676) 1.681–1.685 1.659–1.666 (1.662)	
Nh-L (Shimofukuda)	Nh-L	–	11	38	38.5	11.5	1	6.5	*	2	62	4.5	22	0	1.5	1	0	*	32.5	67	1.495–1.500 (1.499)	1.700–1.707 (1.701–1.702)	–	

Grain composition: Gl., volcanic glass, Rf., rock fragments, Lm., light minerals, Hm., heavy minerals, Ot., other grains, Fl, feldspar, Qz, quartz. Heavy mineral composition: Opx, orthopyroxene, Cpx, clinopyroxene, GHo, green hornblende, BHo, brown hornblende, Cum, cummingtonite, Opq, opaque minerals, Zr, zircon, Bt, biotite, Ap, apatite. Glass-type composition following Yoshikawa (1976): H, H-type shard, C, C-type shard, T, T-type shard, Oth, other type shards. – unidentified, * less than 1%, +++ abundant. References: 1) Yoshikawa *et al.* (1986), 2) Yoshikawa and Inouchi (1991), 3) Katoh *et al.* (1996), and 4) Nomura *et al.* (1995). The BT15 volcanic ash horizon in the Takashima–Ok boring core was correlated with the Sambe Ikeda tephra (SI) by Machida and Arai (1992).

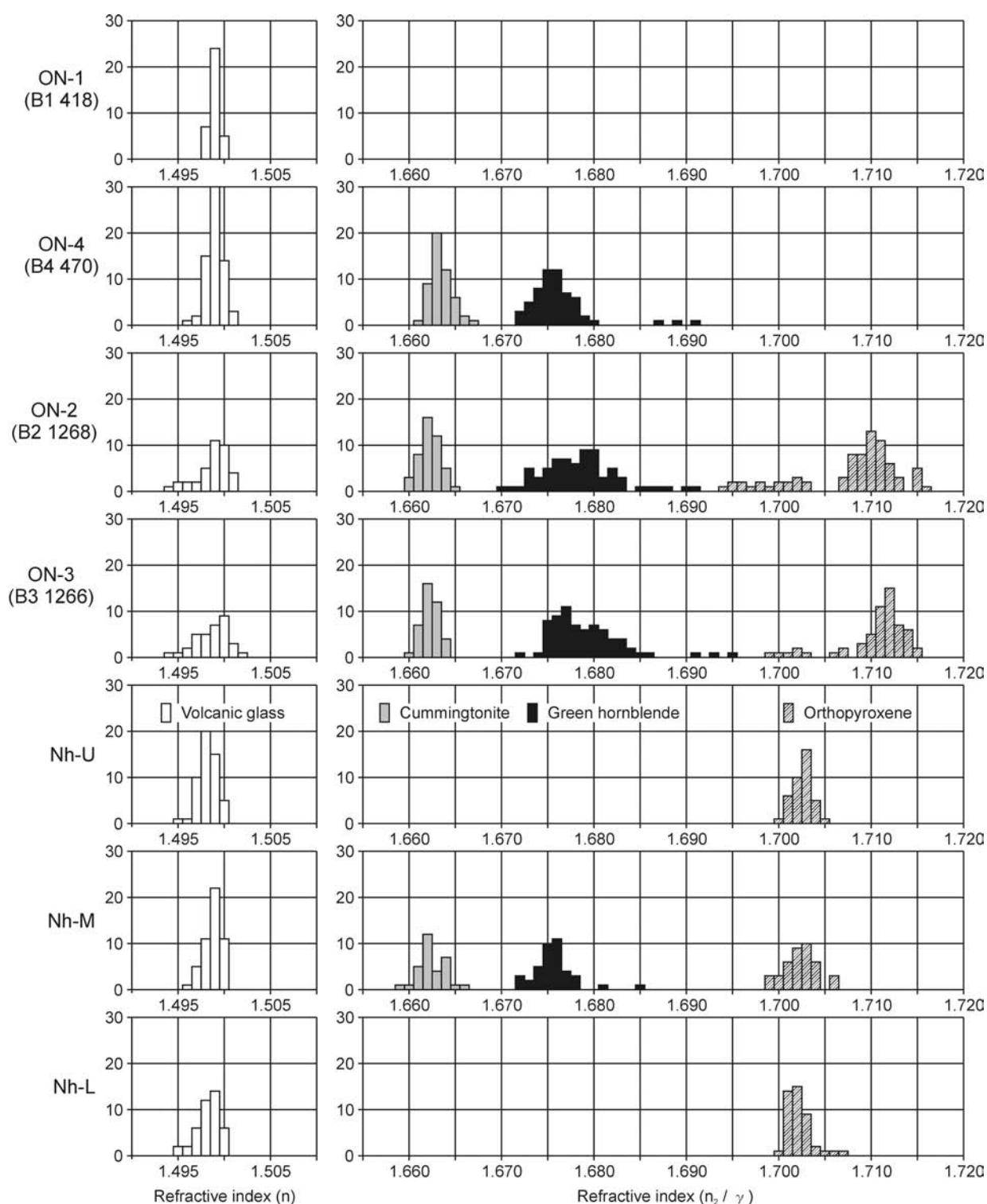


Figure 3. Distributions of refractive indices of volcanic glass shards, and of orthopyroxene, green hornblende, and cummingtonite phenocrysts for two tephra layers newly found in the Ohnuma Moor sediments and the Nh samples taken at Shimofukuda south of Daisen Volcano.

mostly with glass fragments and show the refractive index (n_2) of 1.661–1.667 (1.663) in the ON-4 sample.

Based on the vertical changes in the weight percents of sand fractions, grain and heavy mineral

compositions, and glass shard morphology of the OB-2, OB-3, and OB-5 core sediments, a volcanic horizon corresponding to ON-1 and ON-4 can be detected at 4.79, 4.70, and 4.72 m in depth, respectively (Fig. 4). At these horizons, the sand

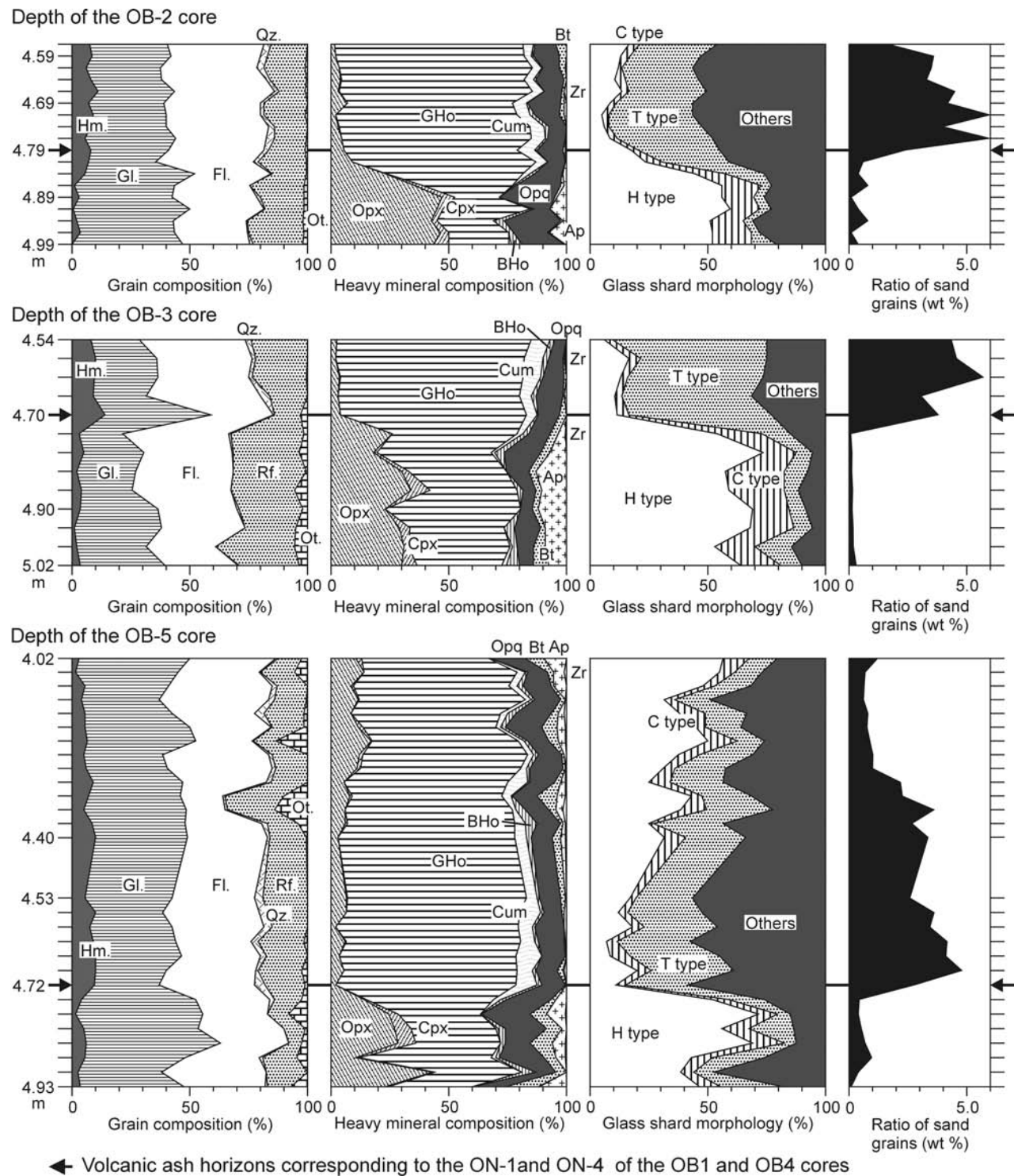


Figure 4. Vertical changes in grain and heavy mineral compositions, glass shard morphology, and weight percents of sand grains in the OB-2, OB-3, and OB-5 cores showing the volcanic ash horizons corresponding to ON-1 and ON-4. See Table 3 for legends of grain and heavy mineral compositions and types of glass shard morphology.

fractions of sediment samples rapidly increase to more than 2.4 wt %, which is 4 to 30 times higher than just below the horizons. Green hornblende and cummingtonite grains also largely increase in the

heavy minerals. More than 2 % of quartz grains appear as light minerals. H-type glass shards are dominant below these levels, while T-type and other type shards become rich in the above sediments.

All evidences indicate the deposition of a volcanic ash layer at these horizons petrographically corresponding to ON-1 and ON-4.

2) ON-2 (12.66-12.68 m in the OB-2 core, 2 cm thick) and ON-3 (12.64-12.66 m in the OB-3 core, 2 cm thick)

These two tephra layers are correlated each other because of their good similarity in petrographic characteristics and stratigraphic positions in both core sediments. They are composed of light mineral grains and glassy rock fragments (> 90 %), with less than 10 % heavy minerals. In ON-2, volcanic glass shards are less than 1 % within all counted grains, and comprise clear H- and T-types, and pale-brown or brown other type shards. Very rare glass shards in ON-3 are mostly composed of colored other type shards. Glass shards of both tephra layers show very concordant refractive indices (n) of 1.494-1.501 (1.499) for ON-2 and 1.492-1.502 (1.500) for ON-3. Heavy mineral compositions are also similar between the two samples. Green hornblende phenocryst (> 70 %) is the commonest in the heavy minerals. Orthopyroxene crystals (5-20 %) are common, and accompanied with a few opaque minerals, apatite, biotite, and cummingtonite crystals less than 5 % each, and rare brown hornblende, clinopyroxene, and zircon grains (at most 1 % each). More than half of green hornblende grains have original shapes with small fragments of glass shard or glassy rock, but most orthopyroxene crystals are weathered to be rounded or to have milled edges. There are some green hornblende grains joining with cummingtonite crystals. As these grains are counted twice as individual minerals, the ratios of green hornblende to cummingtonite crystals are 9.0 (90 to 10) in ON-2, and 15.7 (94 to 6) in ON-3. Refractive index () of orthopyroxene crystals has a very wide range (Fig. 3). Many crystals show the refractive index ranging in 1.705 and 1.716, and a few have the lower refractive index of 1.694-1.703. Most of green hornblende grains have refractive index (n_2) between 1.670 and 1.680 with modes of 1.679-1.680 in ON-2 and 1.677 in ON-3, but very few grains show the higher refractive index of 1.685-1.695. Cummingtonite crystals in both tephra layers indicate almost same refractive index (n_2) of 1.660-1.665 (1.662).

Discussion

Correlation of newly found tephra layers at Ohnuma Moor

1) ON-1 and ON-4 = Sambe Ukinuno Pumice Beds (SUK) = Sakate Volcanic Ash Beds (Sakate)

The ON-1 and ON-4 volcanic ash layers stratigraphically situated between K-Ah and MsP (Fig. 2) show the heavy mineral compositions mainly composed of green hornblende with a small amount of opaque minerals and cummingtonite (Table 3). In the Kinki District, the Sakate tephra (Sakate), a volcanic ash layer between K-Ah and AT, was previously known to have such petrographic properties (Yoshikawa *et al.*, 1986). The Sakate ash beds are correlated with the BT6 volcanic ash horizon in the Takashima-oki boring core (Fig. 1) that was drilled in Lake Biwa and included almost all tephra layers fallen in this district (Yoshikawa and Inouchi, 1991). According to Yoshikawa *et al.* (1986), the Sakate tephra is relatively crystal rich volcanic ash beds with large heavy mineral phenocrysts like amphibole and biotite existing in patches, and consists mainly of light and heavy mineral grains with about 10 % of glass shards (Table 3). A few quartz phenocrysts are included in light minerals. Clear or whitish volcanic glass shards are mainly of C- and T-types and show the refractive index (n) of 1.498-1.503 (1.500). Heavy minerals are mostly composed of amphibole grains with a few biotite crystals. At the BT6 volcanic horizon, a percentage of glass shard increases to 58 % in the grain composition, and that of biotite grains attains to 16 % in the heavy mineral composition (Table 3; Yoshikawa and Inouchi, 1991). Volcanic glass shards are C- and T-types, and other types with refractive index of 1.498-1.501 (1.498-1.500). No distinction of cummingtonite in amphibole phenocrysts, and no data of refractive indices of green hornblende and cummingtonite crystals may decrease the accuracy in correlating both tephra layers. However, stratigraphic positions, grain and heavy mineral compositions, and morphological characteristics and refractive indices of volcanic glass shards, all are very similar between ON-1, ON-4, and Sakate (Table 3). We thus conclude that these tephra layers can be correlated each other.

The Sakate tephra has been correlated with the

distal deposits of SUK by Machida and Arai (2003). Heavy mineral compositions and refractive index of glass shards are, however, different among SUK, Sakate, and their correlatives described in the Chugoku and Kinki Districts (Yoshikawa *et al.*, 1986; Nomura and Tanaka, 1987; Yoshikawa and Inouchi, 1991, 1993; Nomura *et al.*, 1995; Katoh *et al.*, 1996). According to Machida and Arai (2003), refractive index of glass shards in SUK is 1.505-1.507 (1.506). This value is very higher than that of Sakate ($n = 1.498-1.503$). Previous studies described that SUK included no cummingtonite phenocrysts as heavy minerals (e.g. Machida and Arai, 1992). However, Katoh *et al.* (1996) found the tephra layer petrographically very similar to SUK at Kobe City, Hyogo Prefecture, containing a few cummingtonite crystals. They considered that the tephra layer was a distal part of the Sambe Ukinuno pyroclastic-flow deposits (U₁: Matsui and Inoue, 1971) just below SUK, because of a few cummingtonite phenocrysts in the U₁. At contrast, Fukuoka and Matsui (2002) revealed that a few cummingtonite crystals were also included in the matrix of an upper fall-unit of SUK and insisted on the correlation of the tephra layer found at Kobe City to SUK.

As for ON-1 and ON-4, refractive index of glass shards is different from that of SUK (Table 3). Refractive indices (n_2) of green hornblende and cummingtonite crystals of SUK are 1.672-1.678 (1.675) (Katoh *et al.*, 1996) or 1.671-1.675 (1.673) (Machida and Arai, 2003), and 1.660-1.665 (Machida and Arai, 2003), respectively. Petrographic properties except for refractive index of glass shards are thus very similar among ON-1, ON-4, and SUK (Table 3). Moreover, Nomura *et al.* (1995) described that the refractive indices of glass shards for the upper and lower fall-units of SUK were 1.498-1.503 and 1.503-1.507, and suggested the lowering of refractive index of glass shards in the upper unit. Accordingly, refractive index of glass shards is also concordant among ON-1, ON-4, Sakate tephra, and the upper fall-unit of SUK. In these reasons, we conclude that these tephra layers can be correlated each other. Contents of cummingtonite phenocrysts and refractive index of glass shards both change in the fall-units of SUK. Probably, the upper fall-unit of SUK more widely but thinly spread over the central and northern parts of the Kinki District, while the lower fall-unit

deposited thicker in the Chugoku District and in the southwestern part of the Kinki District than in the former two parts.

2) ON-2 and ON-3 = Daisen Nise-hoki Volcanic Ash Beds (Nh)

In the moor deposits at Ohnuma, tephra layers of ON-2 and ON-3 are situated below AT (Fig. 2). In and around this moor, the Daisen Sekigane Pumice Beds of the Daisen Middle Volcanic Ash Formation (DSP: Machida and Arai, 1979) were identified below AT (Katoh *et al.*, 2001). Because of no tephra layers recognized in the moor deposits below ON-2 and ON-3, these tephra layers are considered to be stratigraphically positioned between AT and DSP.

We need to note heavy mineral composition of ON-2, as this tephra layer is recognized as the concentrating horizon of volcanic ash grains that includes many detrital mineral grains as outliers. Most of orthopyroxene crystals with the higher refractive index of 1.705-1.716 are detrital in origin, because many similar orthopyroxene crystals are contained in the sediments just below and above the ON-2 horizon. Fewer orthopyroxene crystals with lower refractive index of 1.694-1.703 are relatively less weathered and considered to be of tephra origin. On the other hand, green hornblende crystals dominating in the heavy minerals show clear original shapes, and more than half of the crystals have glass shard and/or glassy rock covers. Thus, such hornblende crystals are surely of fallout tephra origin. Cumingtonite crystals were also derived from the fallout tephra, because of no existence of cummingtonite crystals in the moor sediments around the ON-2 horizon and of the occurrence of a crystal formed by both green hornblende and cummingtonite. Taking the heavy mineral composition of ON-3 showing an almost pure volcanic ash layer into account (Table 3), it is likely that the original heavy mineral compositions of these two tephra layers consist mostly of green hornblende phenocrysts with small amount of orthopyroxene, opaque mineral, biotite, and apatite grains, accompanied with few cummingtonite and brown hornblende crystals. Representative refractive indices of these tephra layers are considered to be $n = 1.494-1.502$ (1.499-1.500) for glass shards, and $n_2 = 1.670-1.686$ for green hornblende, $n_2 = 1.660-1.665$ (1.662) for cummingtonite, and $n = 1.694-$

1.703 for orthopyroxene crystals (Fig. 3).

The Sambe Ikeda tephra (SI: Machida and Arai, 1992), stratigraphically situated between AT and DSP, is distributed in the Kinki District and shows the heavy mineral composition dominated by green hornblende phenocrysts (Machida and Arai, 2003). Thus, this tephra layer is considered to be one of the correlative candidates to ON-2 and ON-3. However, SI is dominated by pumiceous type glass shards as grains and has the heavy mineral composition rich in biotite grains without orthopyroxene and cummingtonite phenocrysts. Refractive index of green hornblende crystals ranges in 1.670 and 1.676 with a mode of 1.673 (Machida and Arai, 2003). These petrographic properties of SI are different from those of ON-2 and ON-3, showing impossible correlation among them.

On the other hand in the proximal area of Daisen Volcano, Nh is stratigraphically situated between AT and Daisen Kurayoshi Pumice Beds (DKP: Machida and Arai, 1979) and comprises alternating beds of fine pumice, and volcanic sand and ash. Nh is correlative to the Kamogaoka Volcanic Ash Beds (KmA) designated by Tsukui (1984) and known within an area about 20 km east of Daisen Volcano (Okada and Ishiga, 2000). According to Okada (1996) and Okada and Ishiga (2000), heavy minerals in Nh are composed mainly of green hornblende with a small amount of cummingtonite, orthopyroxene, and opaque minerals. The ratio of orthopyroxene in all heavy mineral phenocrysts is the smallest among tephra layers of the Daisen Middle and Upper Volcanic Ash Formations. These characteristics are very similar to those of ON-2 and ON-3, suggesting their correlation. Because the detailed petrographic properties of Nh have been unclear especially for its refractive indices of glass shards and heavy mineral crystals, we analyzed such properties using the samples from Nh at Shimofukuda (Loc.1 in Fig.1), Hiruzen Village, Okayama Prefecture, to confirm the correlation of ON-2 and ON-3 with Nh following the same procedure (Table 3 and Fig. 3).

Dominant light minerals including quartz and 10 to 20 % of glassy rock fragments and heavy mineral grains characterize the grain compositions of Nh at Shimofukuda. More than 90 % of glass shards are other type shards that consist of blocky shards and fragmentary shards sticking to phenocrysts. At least

30 % of pumiceous glass shards of T-type are included in the lower part of Nh. Heavy minerals are composed mainly of green hornblende (50-70 %) with opaque minerals (10-30 %), orthopyroxene (<10 %), cummingtonite (<5 %), small amounts of biotite, apatite, and brown hornblende, and very few clinopyroxene and zircon. Refractive indices are $n = 1.494-1.500$ (1.498-1.499) for glass shards, $n = 1.699-1.707$ (1.700-1.703) for orthopyroxene phenocrysts. In the middle part of Nh, green hornblende and cummingtonite grains show the refractive indices (n_z) of 1.672-1.685 (1.675-1.676) and 1.659-1.666 (1.662), respectively. Co-existing crystal of green hornblende and cummingtonite is also common among ON-2, ON-3, and Nh. The ratios of green hornblende to cummingtonite crystals range from 13.4 (93 to 7) to 19.0 (95 to 5) in Nh in the case of counting such grains belonging to both green hornblende and cummingtonite crystals.

Although slight differences is recognized in contents of opaque mineral and cummingtonite phenocrysts and in modes of refractive indices of orthopyroxene and green hornblende among ON-2, ON-3, and Nh, the petrographic properties are totally similar among them, resulting in the confirmation of their correlation. Accordingly, we conclude that Nh is distributed at Ohnuma Moor about 80 km east of Daisen Volcano. This conclusion contradicts previous studies that the distribution area of Nh was limited to about 20 km eastward from Daisen Volcano (e.g. Okada and Ishiga, 2000). However, most of the late Pleistocene tephra layers erupted from Daisen Volcano like DKP and DSP have elongate distribution areas stretching eastwards (Okada and Ishiga, 2000; Machida and Arai, 2003). It is likely that Nh also has a similar distribution area with a long axis just going through the Ohnuma Moor.

Estimation of the eruption ages of five tephra layers at Ohnuma Moor based on AMS-¹⁴C dates

As the results of tephra correlation in the present paper and Katoh *et al.* (2006), six tephra layers included in the finer sediments about 17-m thick at the Ohnuma Moor were correlated with K-Ah, SUK, MsP, Sh, AT, and Nh in descending stratigraphic order. There was no age estimation of the tephra layers except for K-Ah and AT based on the precise

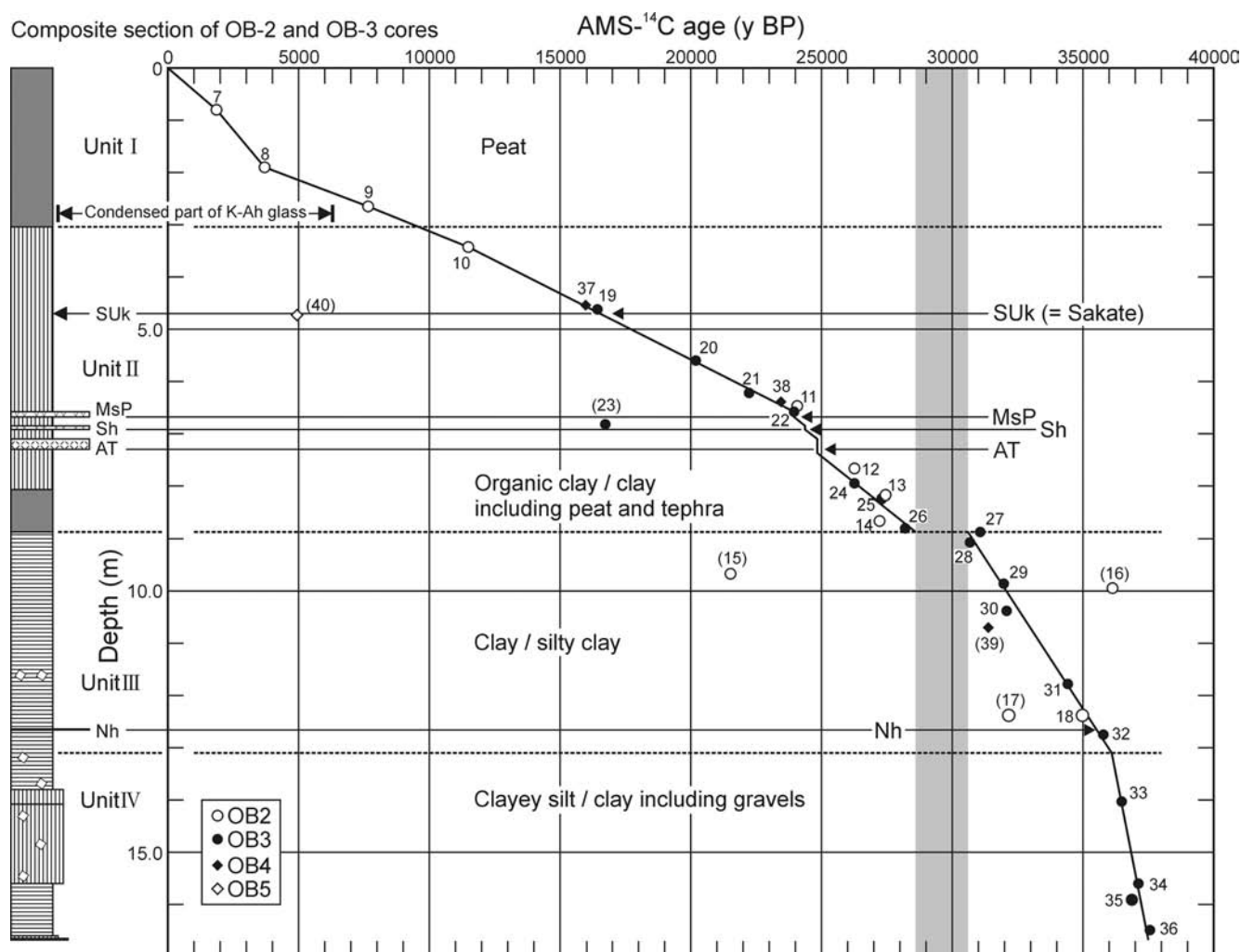


Figure 5. Age-depth model of the Ohnuma Moor sediments shallower than 17.0 m with the horizons of six tephra layers correlated with K-Ah, SUk, MsP, Sh, AT, and Nh, and the 34 AMS-¹⁴C ages from the OB-2 to OB-5 cores.

AMS-¹⁴C dating. We also obtained stratigraphically concordant AMS-¹⁴C ages from the same sediments (Table 2 and Fig. 2) that permit the estimation of eruption ages of SUk, MsP, Sh, and Nh. In addition to these tephra layers, we determine the eruption age of AT and compare it with the previous precise age estimation (Matsumoto *et al.*, 1987; Murayama *et al.*, 1993; Miyairi *et al.*, 2004) to assess our results.

We first made the age-depth model of the sediments at the center of the Ohnuma Moor using 34 AMS-¹⁴C dates from the OB-2 to OB-5 cores (Fig. 5). Because of the detection of SUk in the four cores, we established the composite section of the moor deposits based on the lower boundary of this tephra layer (OB-4) and the correlative volcanic ash horizons (OB-2, OB-3, and OB-5 cores). The OB-2 and OB-3 cores were used for the composite

columnar section above and below the base of SUk, respectively. The length of 1.79 m of the OB-2 core between bases of the uppermost peat and SUk was converted to 1.70 m in this section. The depths of 11 radiocarbon dating horizons in the OB-2 and OB-4 cores were converted in the age-depth model in proportion to the ratios of sediment thickness of both cores to those of the composite section among the peat and four tephra layers of SUk, MsP, AT, and Nh. Original depths (Table 2) were applied to all dating horizons of the OB-3 core, three horizons up to 3.0-m depth in the OB-2 core, and the sample No.39 in the OB-4 core. Converted depth of 4.73 m was determined for the No.40 sample with an original depth of 4.75 m that is 3 cm lower than the base of a volcanic ash horizon correlative to SUk at 4.72 m in the OB-5 core (Fig. 4).

Twelve AMS-¹⁴C ages were determined at ten horizons of the OB-2 core (Nos.7 to 18 in Table 2). Taking error bars (one standard deviation or $\pm 68\%$) of calibrated calendar ages into account, these ages are stratigraphically concordant except for three dates from the clay or silty clay beds between AT and ON-2 (Nos.15, 16, and 17 at 9.73, 10.00, and 12.40 m, respectively) (Table 2 and Fig. 5). The fall of wood fragments from the upper sediments may have resulted in the younger ages of $21,520 \pm 90$ and $32,160 \pm 90$ y BP for the Nos.15 and 17 samples. The radiocarbon age of No.16 ($36,130 \pm 250$ y BP) is much older than those from similar depths (Nos.29 and 30 in Table 2), suggesting the contamination of plant fragments derived from the older sediments around the moor center.

From the OB-3 core for the aim of paleomagnetic secular variation, 18 dating samples were carefully taken at every 18 horizons without picking up contaminant materials. Wood fragments (No.23 in Table 2) just above Sh distinctly show a younger ¹⁴C age compared to the ages obtained from the horizons close to them (Fig. 5). All other dates are concordant stratigraphically under the consideration of their calibrated calendar ages. The weight of the sample No.23 is only 0.25 mg and much smaller than that of all other samples over 0.80 mg. It shows an extraordinarily small ¹³C value of -35.9 ‰ among the measured samples (Table 2). Accordingly, rejuvenation of the radiocarbon age is thought to be due to the contamination of modern carbon during the sample pretreatment.

An AMS-¹⁴C date of wood fragments (No.37 in Table 2; an original depth is 4.54 m), taken from the moor deposits 16 cm above the base of SUk in the OB-4 core, indicated a stratigraphically concordant age, but the sample No.39 distinctly provided a younger age than those from the upper two horizons of Nos. 29 and 30 (Fig. 5). Wood fragments of the OB-5 core at 4.75 m (No.40 in Table 2) show the much younger age largely contradict to the stratigraphic position. Judging from the AMS-¹⁴C age of $4,940 \pm 20$ y BP, the sample should have been mixed within the present horizon from the peat beds above K-Ah by an edge of the sampler. The measurement of paleomagnetic secular variation indicating the disturbance of the OB-5 core sediments confirms this interpretation.

As the results, we can adopt the total of the 28 available AMS-¹⁴C ages to estimate the eruption ages of tephra layers in the moor sediments at Ohnuma: 9 ages from the OB-2 core except for Nos. 15 to 17, 17 ages from the OB-3 core except for No. 23, and 2 ages from the OB-4 core except for No.39. Because one clear hiatus horizon was inferred at around 8.87 m in depth from the changes in sedimentary facies and AMS-¹⁴C dates, the age-depth model curves were figured for individual sedimentary units (Fig. 5). Based mainly on this age-depth model with the 28 available AMS-¹⁴C dates, we interpolate the radiocarbon date of each tephra horizon representing its approximate eruption age on the assumption of a constant sedimentation rate between the two AMS-¹⁴C dating horizons within the same lithostratigraphic units.

1) Nh (12.64-12.66 m in the OB-3 core and 12.66-12.68 m in the OB-2 core)

The eruption age of Nh is calculated using AMS-¹⁴C dates from the OB-3 core. In this core, AMS-¹⁴C dates of $34,420 \pm 140$ y BP and $35,780 \pm 160$ were obtained at 11.78 and 12.75 m just above and below Nh, respectively (Table 2 and Fig. 5). Sedimentation time responsible for the 1 cm thick deposits between these horizons is calculated to be from 11 to 17 y/cm (median: 14 y/cm) taking an error of AMS-¹⁴C dating (one standard deviation) into account. Thus, an age of the base of Nh at 12.66 m can be calculated to be from 35,520 to 35,790 y BP (median: 35,650 y BP). Because the depths of two dated horizons have an error within about 3.0 cm equal to the largest thickness of a sub-sample, 30 to 50 years should be added to or excluded from this estimated age. We thus infer the eruptive age of Nh referable to be $35,650 \pm 200$ y BP (calibrated calendar age of $41,632 \pm 203$ cal. BP using quickcal 2005 ver.1.4.). The estimated eruptive age agrees well with the AMS-¹⁴C date of $34,990 \pm 230$ y BP (No.18 in Table 2) at 12.40 m in the OB-2 core, 28 cm above the base of an identified volcanic ash horizon of Nh (ON-2).

2) AT (7.10-7.37 m in the OB-3 core)

The eruptive age of AT is estimated using the AMS-¹⁴C date of $23,950 \pm 70$ y BP from a wood fragment at 6.58 m in the MsP beds (6.68-6.50 m) and that of $26,270 \pm 80$ y BP from a cone at 7.95 m

below AT in the OB-3 core (Table 2). We consider the very short sedimentation period of AT (27 cm thick) and Sh (7 cm thick) and the constant sedimentation rate of the deposits between the two dated horizons except for these tephra layers. A resultant estimated age of AT is determined to as 24,810 and 24,840 y BP. Taking an error due to sub-sampling (70-80 years) like in the case of Nh into consideration, we present the eruptive age of AT as $24,830 \pm 90$ y BP ($29,858 \pm 274$ cal. BP). This age is concordant with the previously estimated eruptive ages of AT ($24,720 \pm 290$ y BP by Matsumoto *et al.* (1987) by the benzene-liquid scintillation method and $25,120 \pm 270$ y BP by Miyairi *et al.* (2004) by the AMS- ^{14}C dating method) within one standard error, but is slightly older than the age based on the AMS- ^{14}C dating of planktonic foraminiferal tests ($24,330 \pm 230$ y BP by Murayama *et al.*, 1993). Machida and Arai (2003) concluded the radiocarbon ages for AT including AMS- ^{14}C dates by many authors largely ranging from 24,000 to 25,000 y BP.

3) Sh (6.85-6.92 m in the OB-3 core)

The eruptive age of Sh are calculated to be 24,330 to 24,420 y BP (median: 24,370 y BP) by the same procedure as used for the estimation of an eruptive age of AT. It is estimated to be $24,370 \pm 120$ y BP ($29,320 \pm 412$ cal. BP) considering the sub-sampling error of 70 to 80 years.

4) MsP (6.50-6.67 m in the OB-3 core, 6.70-6.54 m in the OB-2 core)

As for MsP, the AMS- ^{14}C dating by wood fragments showed $23,950 \pm 70$ y BP in the pumice beds at 6.58 m in the OB-3 core, and $24,070 \pm 90$ y BP immediately above the MsP horizon at 6.80 m in the OB-2 core (Table 2). These two dates coincide well within one standard error so as to adopt a mean of the two AMS- ^{14}C dates as an eruptive age of MsP, taking their standard errors into account. They suggest that the eruptive age of MsP is $24,010 \pm 150$ y BP ($28,923 \pm 358$ cal. BP).

5) SUK (= Sakate; 4.68-4.70 m in the OB-4 core and 4.70 m in the OB-3 core)

The AMS- ^{14}C date of $15,980 \pm 40$ y BP was obtained at 4.54 m in the OB-4 core 16 cm above ON-4, a correlative of SUK (Table 2). Based on the vertical changes in grain and heavy mineral

compositions of the OB-3 core sediments, the base of a volcanic ash horizon corresponding to the base of ON-4 was detected at 4.70 m (Fig. 4). In the OB-3 core, two AMS- ^{14}C dates of $16,430 \pm 40$ and $20,190 \pm 50$ y BP were taken at 4.62 and 5.60 m, respectively (Table 2). These ages show that the time interval necessary for the 1cm thick sedimentation is calculated to be from 37 to 39 y/cm (median: 38 y/cm) between the two dated horizons. The eruptive age of SUK is thus estimated to be from 16,700 to 16,770 y BP (median: 16,740 y BP). We conclude that the eruptive age of SUK (= Sakate) is $16,740 \pm 160$ y BP ($19,966 \pm 305$ cal. BP) from the effect of the sub-sampling error of 110 to 120 years. This estimated age is also concordant with the AMS- ^{14}C date measured in the OB-4 core.

Summarizing above, the eruptive ages of five tephra layers intercalated in the sediments at Ohnuma Moor, Nh, AT, Sh, MsP, and SUK in ascending stratigraphic order, are estimated to be $35,650 \pm 200$, $24,830 \pm 90$, $24,370 \pm 120$, $24,010 \pm 150$, and $16,740 \pm 160$ y BP, respectively. The estimated eruptive age of AT is not contradict to the previous age estimation (e.g. Machida and Arai, 2003). The eruptive age of Nh has been obtained first in the present paper, and those of Sh, MsP, and SUK can be assessed from the comparison with the previously reported radiocarbon ages.

Nomura and Tanaka (1986) reported that “b volcanic ash layer” in the eastern part of Hyogo Prefecture could be correlated with Sh, Od, or Uh, and they obtained a radiocarbon age of $24,300 \pm 410$ y BP (based on the half-life 5,730 years) from wood fragments just above the volcanic ash beds by the usual gas proportional counting. According to the petrographic properties of major tephra layers of the Daisen Upper Volcanic Formation described by Katoh *et al.* (2004), the “b volcanic ash layer” can be correlated with Sh because of no content of cummingtonite phenocrysts. Therefore, the above radiocarbon age (re-calculated to be $23,610 \pm 400$ y BP using Libby half-life 5,568 years) suggests the upper limit of an eruptive age of Sh and confirms our age estimation for Sh ($24,370 \pm 120$ y BP).

Three radiocarbon dates of $16,000 \pm 400$ y BP (Matsui and Inoue, 1970), $14,780 \pm 400$ y BP (Hattori *et al.*, 1983), and $16,400 \pm 140$ y BP (Miura and Hayashi, 1991) were obtained from charcoals contained in the U₁ pyroclastic-flow deposits

immediately below SUK. On the basis of the first radiocarbon date, SUK was considered to have erupted from 15,000 to 16,000 y BP (Matsui and Inoue, 1971). Recently, Fukuoka (2005) reported three more radiocarbon dates of $16,050 \pm 80$, $15,880 \pm 70$, and $15,940 \pm 80$ y BP for the U_1 deposits. In addition to these dating on the proximal pyroclastic-flow deposits, the peaty silt beds just above and below the volcanic ash layer formerly correlated to the distal deposit of U_1 were dated to be $15,740 \pm 80$ and $15,490 \pm 120$ y BP, respectively (Kato et al., 1996). Moreover, Nomura et al. (1995) inferred the eruptive age of SUK just after a radiocarbon age of $15,800 \pm 250$ y BP (based on the half-life 5,730 years). From these radiocarbon dates by the measurement of beta emission, the eruptive age of SUK is considered to be around 16,000 y BP. Our estimated age of SUK ($16,740 \pm 160$ y BP) is slightly older than most of the previous radiocarbon dates obtained for the U_1 deposits by the beta emission counting method, but is consistent in considering the different dating methods and the larger error of their calibrated calendar ages around 16,000 y BP.

Nomura et al. (1995) inferred that MsP erupted just after the radiocarbon age of $17,400 \pm 1,080$, -960 y BP (based on the half-life 5,730 years) measured for the organic silt beds just above MsP by the beta emission counting method. The radiocarbon ages by the gas proportional counting of $16,200 \pm 360$ and $18,600 \pm 205$ y BP (both based on the half-life 5,730 years) were taken from the organic clay and peat beds just above and below MsP, respectively, in the eastern part of Hyogo Prefecture (Nomura and Tanaka, 1986), and the estimated eruptive age of MsP is almost equal to the mean of these two radiocarbon dates (Nomura et al., 1995). According to their results based on the measurement of beta emission, the eruptive age of MsP is considered to be between 16,000 and 18,500 y BP younger than our estimation of $24,010 \pm 150$ y BP by 5,300 to 8,200 years. Radiocarbon dates concerning to the AT eruption by the AMS- ^{14}C dating method are generally 2,000 to 3,000 years older than those determined by the beta emission measurement (Machida and Arai, 2003). However, the larger difference between the two estimated eruption ages of MsP cannot be explained only by the different dating techniques.

Around Daisen Volcano, the Kusadanihara

Pumice Beds (KsP: Tsukui, 1984) underlies the Misen pyroclastic-flow deposits (MiF: Tsukui, 1984) and is stratigraphically situated above MsP. A radiocarbon age of $18,100 \pm 180$ y BP determined by the beta emission measurement from charcoals in MiF possibly shows the eruption of KsP around 18,000 y BP (Miura and Hayashi, 1991). The eruptive age of KsP has recently supported by the AMS- ^{14}C dating using planktonic foraminiferal tests deposited on the ocean floor of Japan Sea (Domitsu et al., 2002). Therefore, the estimated eruptive age of MsP by Nomura et al. (1995), which is recalculated to be $16,910 \pm 1,050$, -930 y BP based on Libby half-life 5,568 years, is almost equal to or slightly younger than the eruptive age of KsP.

Nomura et al. (1995) correlated the "Hs-4" and "Hs-9" tephra layers at Hosoiike Moor in the Chugoku Mountains (Fig. 1) with MsP and obtained the radiocarbon date of $17,400 \pm 1,080$, -960 y BP from the organic silt beds just above the "Hs-4" tephra horizon. The "Hs-9" immediately overlies the "Hs-10" (= Uh) and "Hs-11" (= AT) tephra layers at this moor like the stratigraphy of MsP, Uh, and AT found around Daisen Volcano, in spite of no identification of Uh and AT below the "Hs-4". The stratigraphy of "Hs-9" relative to Uh and AT suggest the small time gap among the eruptions of these tephra layers, but it is inconsistent with their estimated eruption age of MsP indicating at least 6,000 years passage after the AT eruption. The "c volcanic ash layer" correlated to MsP in eastern Hyogo have no description of cummingtonite phenocrysts as heavy minerals (Nomura and Tanaka, 1986). Above MsP, the Daisen Kagamiganaru tephra layer (DKg: Machida and Arai, 1979) and KsP show very similar petrographic properties to MsP except for the occurrence of cummingtonite phenocrysts in MsP (Machida and Arai, 2003). SUK also has the similar petrographic characteristics with the "c volcanic ash layer", although the latter contains more orthopyroxene phenocrysts.

Correlation of the "Hs-4" and the "c volcanic ash layer" with MsP is difficult only based on the petrographic description by Nomura et al. (1995) and Nomura and Tanaka (1986), respectively. Their petrographic characteristics and estimated eruptive ages also suggest the possible correlation of the "Hs-4" and the "c volcanic ash layer" with KsP or DKg. Furthermore, sedimentation rate above the "c volcanic ash layer" is extraordinarily small, because

the peaty layer 30 cm above the “c volcanic ash layer” was dated to be $11,700 \pm 95$ y BP (based on the half-life 5,730 years) by the beta emission counting method. This may be due to the contamination of modern carbon into the dated peaty beds near the ground surface. Accordingly, it is likely that the previous estimated eruption age of MsP (around 17,400 y BP) is younger because of the miscorrelation of a dated tephra layer and/or the effect of modern carbon contaminating into the dated materials used for the age estimation.

Conclusion

Four tephra layers of the Kikai-Akahoya tephra (K-Ah), Aira-Tn tephra (AT), Daisen Shitano-hoki Volcanic Ash Beds (Sh), and Daisen Misen Pumice Beds (MsP) are included in the uppermost part of the moor deposits at Ohnuma Moor in the eastern part of the Chugoku Mountains, northern Hyogo Prefecture. In addition to these tephra layers, two thin volcanic ash layers were newly identified in the moor deposits below AT and between K-Ah and MsP. These tephra layers were correlated with the Daisen Nise-hoki Volcanic Ash Beds (Nh) of the Daisen Middle Volcanic Ash Formation and the Sakate tephra layer (Sakate) that was known to be widespread in the Kinki District, respectively. The Sakate tephra was also correlated herein to the upper unit of the Sambe Ukinuno Pumice Beds (SUK) erupted from Sambe Volcano. The tephra correlation revealed that Nh was distributed in an area about 80 km east of Daisen Volcano and confirmed that SUK was widespread at least in the central and northern parts of the Kinki District, Japan.

The eruptive ages of Nh, AT, Sh, MsP, and SUK were estimated using the available 28 AMS- ^{14}C dates from the sediments up to 17.0 m in depth at the Ohnuma Moor. By interpolating the radiocarbon date of a tephra horizon as its eruption age on the assumption of a constant sedimentation rate between the two AMS- ^{14}C dating horizons, the eruptive ages of Nh, AT, Sh, MsP, and SUK were estimated to be $35,650 \pm 200$, $24,830 \pm 90$, $24,370 \pm 120$, $24,010 \pm 150$, and $16,740 \pm 160$ y BP, respectively. The estimated ages of AT, Sh, and SUK are almost concordant with the previously estimated ages, but the eruptive age of MsP is 5,300 to 8,200 years older than the previous one. The large difference in

age determination may result from the miscorrelation of the dated tephra with MsP and/or the effect of modern carbon contaminating into the dated materials in the previous studies.

Acknowledgements

Two anonymous reviewers and the editor Prof. F. Kobayashi provided us with helpful comments and discussions. The technicians of Tanaka Geological Company, especially T. Nonaka, T. Uekita, and T. Besho, conducted the boring work at Ohnuma Moor under heavy snow. Dr. E. Niwa helped the sample preparation for AMS- ^{14}C dating at the Center for Chronological Research, Nagoya University. Dr. S. Kodate of Institute of Natural and Environmental Sciences, University of Hyogo, introduced us some references concerning to the vegetation of the Ohnuma Moor. The Japan Ministry of Education, Science, Sports and Culture provided financial support for this work to S. Katoh (No. 14380034) from 2002 to 2005. We thank all of these individuals and organizations for their sincerely assistance.

References

- Danhara, T., 1993.** An improved system for measuring refractive index using thermal immersion method. In Japan Association for Quaternary Research (ed.), *A hand book of Quaternary Research 2*, University of Tokyo Press, Tokyo, pp.149-157. (In Japanese, title translated)
- Danhara, T., Yamashita, T., Iwano, H. and Kasuya, M., 1992.** An improved system for measuring refractive index using thermal immersion method. *Quaternary International*, **13/14**: 89-91.
- Domistu, H., Shiihara, M., Torii, M., Tsukawaki, S. and Oda, M., 2002.** Tephrostratigraphy of the piston cored sediment KT96-17 P-2 in the southern Japan Sea—the eruption age of Daisen-Kusadanihara Pumice (KsP)—. *Journal of the Geological Society of Japan*, **108**: 545-556. (In Japanese with English abstract)
- Fukuoka, T., 2005.** ^{14}C ages of the Stage IV pyroclastic deposits at Sanbe Volcano. *Bulletin of the Shimane Nature Museum of Mt. Sanbe (Sahimel)*, **3**: 61-64. (In Japanese with English

abstract)

- Fukuoka, T. and Matsui, S., 2002.** Stratigraphy of pyroclastic deposits post-dating the AT tephra, Sanbe Volcano. *Earth Science* (Chikyu Kagaku), **56**: 105-122. (In Japanese with English abstract)
- Furuyama, K., Nagao, K., Mitsui, S. and Kasatani, K., 1993.** K-Ar ages of Late Neogene mono-genetic volcanoes in the east San-in District, Southwest Japan. *Earth Science* (Chikyu Kagaku), **47**: 519-532.
- Hattori, H., Shikano, K., Suzuki, T., Yokoyama, S., Matsuura, H. and Sato, H. 1983.** *Geology of the Sambesan District, with geological sheet map at 1:50,000*. Geological Survey of Japan, Tsukuba, 168 p. (In Japanese with English abstract)
- Kamata, H., Danhara, T., Yamashita, T., Hoshizumi, H., Hayashida, A. and Takemura, K., 1994.** Correlation of the Azuki Volcanic Ash of the Osaka Group and the Ku6C Volcanic Ash of the Kazusa Group to the Imaichi pyroclastic-flow deposit in central Kyushu, Japan—A co-ignimbrite ash erupted from Shishimuta caldera—. *Journal of the Geological Society of Japan*, **100**: 848-866. (In Japanese with English abstract)
- Katoh, S., 2005.** A new method of taking undisturbed all-cored sediment samples with a constant direction for the analysis of paleomagnetic secular variation (PSV). In *Research on Active Faulting and Mitigate Seismic Hazards: the State of the Art*, Abstracts of the HOKUDAN International Symposium on Active Faulting 2005, Hokudan, pp. 63.
- Katoh, S., Danhara, T., Yamashita, T., Takemura, K. and Okada, A., 1996.** Late Quaternary tephra layer derived from Sanbe Volcano discovered in Kobe City, western Japan. *The Quaternary Research*, **35**: 383-389. (In Japanese with English abstract)
- Katoh, S., Morinaga, H., Danhara, T., Yamashita, T., Kobayashi, F., Sato, H., Handa, K., Furutani, H., Sakiyama, T. and Yagi, T., 2006.** Late Pleistocene development of the Ohnuma Moor in the eastern part of the Chugoku Mountains, western Japan. In Katoh, S. (ed.), *High-resolution reconstruction of the paleoenvironmental changes since the Last Glacial by the analyses of highland moor deposits*. Report to the Japan Society for Promotion of Science, Tokyo, pp. 12-28. (In Japanese with English abstract)
- Katoh, S., Ohmori, H., Matsuda, T., Yamashita, T., Danhara, T., Sakiyama, T., Handa, K., Sato, H., Furutani, H. and Kobayashi, F., 2001.** Late Quaternary tephrostratigraphy around Mt. Hachibuse in northwestern Hyogo Prefecture, with special reference to tephra layers from Daisen Volcano. *Humans and Nature*, **12**: 1-12. (In Japanese with English abstract)
- Katoh, S., Yamashita, T. and Danhara, T., 2004.** Correlation among the tephra layers in the Lowest Daisen Volcanic Ash Formation, western Japan, on the basis of their petrographic properties. *The Quaternary Research*, **43**: 435-445. (In Japanese with English abstract)
- Machida, H. and Arai, F., 1976.** Widespread volcanic ash layer—Discovery of the Aira-Tn volcanic ash layer and its significance—. *Kagaku*, **46**: 339-347. (In Japanese, title translated)
- Machida, H. and Arai, F., 1978.** Akahoya Ash—A Holocene widespread tephra erupted from the Kikai Caldera, south Kyushu, Japan. *The Quaternary Research*, **17**: 143-163 (In Japanese with English abstract)
- Machida, H. and Arai, F., 1979.** Daisen Kurayoshi Pumice: Stratigraphy, chronology, distribution and implication to Late Pleistocene events in Central Japan. *Japanese Journal of Geography*, **88**: 33-50. (In Japanese with English abstract)
- Machida, H. and Arai, F., 1992.** *Atlas of tephra in Japan and its surrounding area*. University of Tokyo Press, Tokyo, 276p. (In Japanese, title translated)
- Machida, H. and Arai, F., 2003.** *Atlas of tephra in Japan and its surrounding area, 2nd edition*. University of Tokyo Press, Tokyo, 336p. (In Japanese, title translated)
- Matsui, S. and Inoue, T., 1970.** ^{14}C age of Ejecta of Sanbe Volcano— ^{14}C age of the Quaternary deposits in Japan (56)—. *Earth Science* (Chikyu Kagaku), **24**: 112-114. (In Japanese)
- Matsui, S. and Inoue, T., 1971.** Pyroclastics and their stratigraphy from Volc. Sanbe. *Earth Science* (Chikyu Kagaku), **25**: 147-163. (In Japanese with English abstract)
- Matsumoto, E., Maeda, Y., Takemura, K. and Nishida, S., 1987.** New radiocarbon age of Aira-Tn Ash (AT). *The Quaternary Research*, **26**: 79-83. (In Japanese with English abstract)

- Miura, K. and Hayashi, M., 1991.** Quaternary tephra studies in the Chugoku and Shikoku Districts. *The Quaternary Research*, **30**: 339-351. (In Japanese with English abstract)
- Miyairi, Y., Yoshida, K., Miyazaki, Y., Matsuzaki, H. and Kaneoka, I., 2004.** Improved ^{14}C dating of a tephra layer (AT tephra, Japan) using AMS on selected organic fractions. *Nuclear Instruments and Methods in Physics Research B*, **223-224**: 555-559.
- Miyoshi, N. and Yano, N., 1986.** Late Pleistocene and Holocene vegetational history of the Ohnuma Moor in the Chugoku Mountains, western Japan. *Review of Paleobotany and Palynology*, **46**: 355-376.
- Murayama, M., Matsumoto, E., Nakamura, T., Okamura, M., Yasuda, H. and Taira, A., 1993.** Reexamination of the eruption age of Aira-Tn ash (AT) obtained from a piston core off Shikoku—determined by AMS ^{14}C dating of planktonic foraminifera. *Journal of the Geological Society of Japan*, **99**: 787-798. (In Japanese with English abstract)
- Nomura, R. and Tanaka, S., 1986.** The tephra layers derived from Daisen Volcano found in the Sasayama Basin and its vicinity, Hyogo Prefecture. *The Quaternary Research*, **24**: 301-307. (In Japanese)
- Nomura, R. and Tanaka, S., 1987.** U₂ Volcanic Ash Beds in southern Hyogo Prefecture—Its correlation and implication to chronology of landforms—. *Ron-shu* (Journal of Liberal Arts, Kobe University), **39**: 1-20. (In Japanese, title translated)
- Nomura, R., Tanaka, S., Kashiwaya, K., Soma, H., Ogura, H. and Kawasaki, T., 1995.** Stratigraphic and petrographic properties of the tephra layers in Hosoiike Moor, Okayama Prefecture, Japan. *The Quaternary Research*, **34**: 1-8. (In Japanese with English abstract)
- Okada, S., 1996.** Daisen Hiruzenbara Pumice (DHP) and hpm2 Pumice erupted from the Daisen Volcano. *Geoscience Report of Shimane University*, **15**: 53-60. (In Japanese with English abstract)
- Okada, S. and Ishiga, S., 2000.** Tephra from Daisen Volcano. In Sawada, Y. and Nomura, N. (ed.), *Field Excursion Guidebook of the 107th Annual Meeting of the Geological Society of Japan*, Matsue, 81-90. (In Japanese)
- Okada, S. and Tanimoto, S., 1986.** On two pumice fall beds discovered in the Daisen Lower Tephra Member. *Journal of Faculty of Education, Tottori University, Natural Science*, **35** (1-2): 33-42. (In Japanese with English abstract)
- Sakiyama, T., Matsuda, T., Morinaga, H., Goto, A. and Katoh, S., 1995.** Pliocene to Pleistocene volcanic rocks in northern Hyogo Prefecture, southwest Japan. —K-Ar age, paleomagnetism and major elements—. *Humans and Nature*, **6**: 149-170. (In Japanese with English abstract)
- Takenaka, N. and Kojima, M., 1987.** The moor vegetation of Hyogo Prefecture IV. Ohnuma Moor. In *Papers on plant ecology and taxonomy to the memory of Dr. Satoshi Nakanishi*, The Kobe Geobotanical Society, Kobe, pp.147-163. (In Japanese with English abstract)
- Tsukui, M., 1984.** Geology of Daisen Volcano. *Journal of the Geological Society of Japan*, **90**: 643-658. (In Japanese with English abstract)
- Yoshikawa, S., 1976.** The volcanic ash layers of the Osaka Group. *Journal of the Geological Society of Japan*, **82**: 497-515. (In Japanese with English abstract)
- Yoshikawa, S. and Inouchi, Y., 1991.** Tephrostratigraphy of the Takashima-oki boring core samples from Lake Biwa, central Japan. *Earth Science* (Chikyu Kagaku), **45**: 81-100. (In Japanese with English abstract)
- Yoshikawa, S. and Inouchi, Y., 1993.** Middle Pleistocene to Holocene explosive volcanism revealed by ashes of the Takashima-oki core samples from Lake Biwa, central Japan. *Earth Science* (Chikyu Kagaku), **47**: 97-109. (In Japanese with English abstract)
- Yoshikawa, S., Nasu, T., Taruno, H. and Furutani, M., 1986.** Late Pleistocene to Holocene volcanic ash layers in Central Kinki District, Japan. *Earth Science* (Chikyu Kagaku), **40**: 18-38 (In Japanese with English abstract)

Received: August 9, 2006

Accepted: December 28, 2006